Lecture Notes on Advances of Numerical Methods for Hubbard Quantum Monte Carlo Simulation

4 authors, including:

Wenbin Chen
Fudan University
95 PUBLICATIONS **1,082** CITATIONS

SEE PROFILE

Ichitaro Yamazaki
University of Tennessee
94 PUBLICATIONS **803** CITATIONS

SEE PROFILE

Lecture Notes on Advances of Numerical Methods for Hubbard Quantum Monte Carlo Simulation

Part 1, July 30, 2007

Zhaojun Bai
Wenbin Chen
Richard Scalettar
Ichitaro Yamazaki

Contents

Lecture 1

Hubbard model and QMC simulations

1.1 Introduction

The Hubbard model is a fundamental model to study one of the core problems in materials science: How do the interactions between electrons in a solid give rise to properties like magnetism, superconductivity, and metal-insulator transitions? In this lecture, we introduce the Hubbard model and outline quantum Monte Carlo (QMC) simulation to study many-electron systems. Subsequent lectures will describe computational kernels of the QMC simulation.

1.2 Hubbard model

The two-dimensional Hubbard model for simulating the interactions between electrons is defined by the Hamiltonian ([7, 8]):

$$\mathcal{H} = \mathcal{H}_K + \mathcal{H}_\mu + \mathcal{H}_V, \tag{1.2.1}$$

where $\mathcal{H}_K$, $\mathcal{H}_\mu$ and $\mathcal{H}_V$ stand for kinetic energy, chemical energy and potential energy, respectively, and are defined as

$$\begin{aligned} \mathcal{H}_K &= -t \sum_{\langle i,j\rangle,\sigma} (c^\dagger_{i\sigma} c_{j\sigma} + c^\dagger_{j\sigma} c_{i\sigma}), \\ \mathcal{H}_\mu &= -\mu \sum_i (n_{i\uparrow} + n_{i\downarrow}) \\ \mathcal{H}_V &= U \sum_i (n_{i\uparrow} - \frac{1}{2})(n_{i\downarrow} - \frac{1}{2}) \end{aligned}$$

and

- i and j label the spatial sites of the lattice. $\langle i, j\rangle$ represents the electrons only hopping to nearest neighboring sites.
- the operators $c^\dagger_{i\sigma}$ and $c_{i\sigma}$ are the fermion creation and annihilation operators for electrons located on the ith lattice site with z component of spin $\sigma = \uparrow$(up) or $\downarrow$(down), respectively.
- The operators $n_{i\sigma} = c^\dagger_{i\sigma} c_{i\sigma}$ are the number operators which count the number of electrons of spin σ on site i.

- t is a hopping parameter for the kinetic energy of the electrons, and is determined by the overlap of atomic wave functions on neighboring sites,
- The term $Un_{i\uparrow}n_{i\downarrow}$ represents an energy cost U for the site i has two electrons. It describes a local repulsion between electrons, referred to as Coulomb interaction.
- μ is the chemical potential parameter which controls the electronic numbers (or density).

Note that the kinetic energy $\mathcal{H}_K$ and chemical potential energy $\mathcal{H}_\mu$ are quadratic in creation and destruction operators. The potential energy $\mathcal{H}_V$ is quartic.

The expected value of a physical observable $\mathcal{E}$ of interest, such as density-density correlation, spin-spin correlation or magnetic susceptibility, is given by

$$\langle \mathcal{E} \rangle = \mathrm{Tr}(\mathcal{E}\mathcal{P}), \tag{1.2.2}$$

where $\mathcal{P}$ is a distribution operator defined as

$$\mathcal{P} = \frac{1}{\mathcal{Z}} e^{-\beta \mathcal{H}}, \tag{1.2.3}$$

and $\mathcal{Z}$ is referred to as the partition function defined as

$$\mathcal{Z} = \mathrm{Tr}(e^{-\beta \mathcal{H}}), \tag{1.2.4}$$

and β is proportional to the inverse of the prodcut of the Boltzmann's constant k_B and the temperature T, i.e.,

$$\beta = \frac{1}{k_B T}.$$

Therefore, β is called an *inverse temperature*, in short.

"Tr" is a trace over the Hilbert space describing all the possible occupation states of the lattice:

$$\mathrm{Tr}(e^{-\beta \mathcal{H}}) = \sum_i \langle \psi_i | e^{-\beta \mathcal{H}} | \psi_i \rangle,$$

where $\{|\psi_i\rangle\}$ is an orthonormal basis of the Hilbert space. Note that the trace does not depend on the choice of the basis. A choice of the basis is the so-called "occupation number basis (local basis)" as described below.

In a classical problem where $\mathcal{H} = E$ is the energy, a real variable, then $\exp(-\beta E)/Z$ is the probability, where $Z = \int e^{-\beta E}$. In quantum mechanics, as we shall see, we will need to recast the operator $\exp(-\beta \mathcal{H})$ into a real number. The "path integral representation" of the problem to do this was introduced by Richard Feynman.

Remark **1.2.1** *The creation operators $c^\dagger_{i\sigma}$ and the annihilation operators $c_{i\sigma}$ have the anticommutation relations:*

$$\begin{aligned} \{c_{j\sigma}, c^\dagger_{\ell\sigma'}\} &= \delta_{j\ell}\delta_{\sigma\sigma'}, \\ \{c^\dagger_{j\sigma}, c^\dagger_{\ell\sigma'}\} &= 0, \\ \{c_{j\sigma}, c_{\ell\sigma'}\} &= 0, \end{aligned}$$

where the anticommutator of two operators a and b is defined by $ab+ba$, i.e. $\{a,b\}=ab+ba$. $\delta_{j\ell}$ is the common δ-notation, i.e., $\delta_{j\ell}=1$ if $j=\ell$, and otherwise, $\delta_{j\ell}=0$.

If we choose $j=\ell$ and $\sigma=\sigma'$ in the second anticommutation relation, we conclude that $(c^\dagger_{j\sigma})^2=0$. That is, one cannot create two electrons on the same site with the same spin (Pauli exclusion principle). Thus the anticommutation relations imply the Pauli principle. If the site or spin indices are different, the anticommutation relations tell us that exchanging the order of the creation (or destruction) of two electrons introduces a minus sign. In this way the anticommutation relations also guarantee that the wave function of the particles being described is antisymmetric, another attribute of electrons (fermions). Bosonic particles (which have symmetric wave functions) are described by creation and destruction operators which commute.

Remark **1.2.2** *According to Pauli exclusion principle of electrons, there are four possible states at every site:*

$|\cdot\rangle$ *no particle,*
$|\uparrow\rangle$ *one particle with spin up,*
$|\downarrow\rangle$ *one particle with spin down,*
$|\uparrow\downarrow\rangle$ *two particles with different spin directions.*

Therefore the dimension of the Hilbert space is 4^N, where N is the number of sites.

A second quantization is also used to describe the states if the spin-direction is omitted:

$|0\rangle$: *no particle,*
$|1\rangle$: *one particle.*

The actions of the basic operators on the states are (here we omit the i,σ indices):

$$\begin{array}{lll} c: & |0\rangle=0, & |1\rangle=|0\rangle, \\ c^\dagger: & |0\rangle=|1\rangle, & |1\rangle=0, \\ n: & |0\rangle=0, & |1\rangle=|1\rangle. \end{array} \tag{1.2.5}$$

The last equation of (1.2.5) shows that the states $|0\rangle$ and $|1\rangle$ are the eigen-states of the number operator $n=c^\dagger c$.

Remark **1.2.3** *The operator $n_\uparrow n_\downarrow$ describes the potential energy of two electrons with different spin directions at the same site:*

$$\begin{array}{lll} n_\uparrow n_\downarrow: & |\cdot\rangle=0, & |\uparrow\rangle=0, \\ & |\downarrow\rangle=0, & |\uparrow\downarrow\rangle=|\uparrow\downarrow\rangle, \end{array} \tag{1.2.6}$$

and

$$\begin{array}{lll} U(n_\uparrow-\frac{1}{2})(n_\downarrow-\frac{1}{2}): & |\cdot\rangle=+\frac{U}{4}|\cdot\rangle, & |\uparrow\rangle=-\frac{U}{4}|\uparrow\rangle, \\ & |\downarrow\rangle=-\frac{U}{4}|\downarrow\rangle, & |\uparrow\downarrow\rangle=+\frac{U}{4}|\uparrow\downarrow\rangle. \end{array} \tag{1.2.7}$$

These eigenenergies immediately illustrate a key aspect of the physics of the Hubbard model: The single occupied states $|\uparrow\rangle$ and $|\downarrow\rangle$ are lower in energy by U (and hence more likely to occur). These states are the ones which have nonzero magnetic moment $m^2=(n_\uparrow-n_\downarrow)^2$. One therefore says that the Hubbard interaction U favors the presence of magnetic moments. As we shall see, a further question (when t is nonzero) is whether these moments will order in special patterns from site to site.

Remark **1.2.4** *The operator $c_i^\dagger c_{i+1}$ describes the kinetic energy of the electrons on nearest neighbor sites:*

$$\begin{aligned} c_i^\dagger c_{i+1}: \quad & |00\rangle = 0, \quad |01\rangle = |10\rangle, \\ & |10\rangle = 0, \quad |11\rangle = c_i^\dagger |10\rangle = 0. \end{aligned}$$

Therefore, if there is one particle on the $i+1$th site, and no particle on the ith site, the operator $c_i^\dagger c_{i+1}$ destroies the particle on the $i+1$th site and create one particle on the ith site. We say the electron hops from site $i+1$ to site i after the action of the operator $c_i^\dagger c_{i+1}$.

1.2.1 Hubbard model with no hopping

Let us consider a special case of the Hubbard model, namely, there is only one site and no hopping, i.e., $t = 0$. Then the Hamiltonian $\mathcal{H}$ is

$$\mathcal{H} = U(n_\uparrow - \frac{1}{2})(n_\downarrow - \frac{1}{2}) - \mu(n_\uparrow + n_\downarrow).$$

It can be immediately verified that the orthonormal eigen-states ψ_i of the operator n_σ are also the eigen-states of the Hamiltonian $\mathcal{H}$:

$$\begin{aligned} \mathcal{H}|\cdot\rangle &= \frac{U}{4}|\cdot\rangle, \\ \mathcal{H}|\uparrow\rangle &= \left(\frac{U}{4} - (\mu + \frac{U}{2})\right)|\uparrow\rangle, \\ \mathcal{H}|\downarrow\rangle &= \left(\frac{U}{4} - (\mu + \frac{U}{2})\right)|\downarrow\rangle, \\ \mathcal{H}|\uparrow\downarrow\rangle &= \left(\frac{U}{4} - 2\mu\right)|\uparrow\downarrow\rangle. \end{aligned}$$

The Hamiltonian $\mathcal{H}$ is diagonalized under the basis $\{\psi_i\}$:

$$\mathcal{H} \longrightarrow \left(\langle\psi_i|\mathcal{H}|\psi_j\rangle\right) = \begin{bmatrix} \frac{U}{4} & & & \\ & \frac{U}{4} - \left(\mu + \frac{U}{2}\right) & & \\ & & \frac{U}{4} - \left(\mu + \frac{U}{2}\right) & \\ & & & \frac{U}{4} - 2\mu \end{bmatrix}.$$

Consequently, the operator $e^{-\beta\mathcal{H}}$ is diagonalized:

$$e^{-\beta\mathcal{H}} \longrightarrow e^{-\frac{U\beta}{4}} \mathrm{diag}\left(1, e^{\beta(U/2+\mu)}, e^{\beta(U/2+\mu)}, e^{2\mu\beta}\right).$$

The partition function $\mathcal{Z}$ becomes

$$\mathcal{Z} = \mathrm{Tr}(e^{-\beta\mathcal{H}}) = \sum_i \langle\psi_i|e^{-\beta\mathcal{H}}|\psi_i\rangle \longrightarrow Z = e^{-\frac{U\beta}{4}}\left(1 + 2e^{\left(\frac{U}{2}+\mu\right)\beta} + e^{2\mu\beta}\right).$$

The related operators $\mathcal{H}e^{-\beta\mathcal{H}}$, $n_\uparrow e^{-\beta\mathcal{H}}$, $n_\downarrow e^{-\beta\mathcal{H}}$ and $n_\uparrow n_\downarrow e^{-\beta\mathcal{H}}$, as necessary for calculating physical observables $\mathcal{E}$ of interest, become

$$\begin{aligned}
\mathcal{H}e^{-\beta\mathcal{H}} &\rightarrow e^{-\frac{U\beta}{4}}\mathrm{diag}\left(\frac{U}{4},(-\mu-\frac{U}{4})e^{\beta(U/2+\mu)},(-\mu-\frac{U}{4})e^{\beta(U/2+\mu)},(\frac{U}{4}-2\mu)e^{2\mu\beta}\right)\\
n_\uparrow e^{-\beta\mathcal{H}} &= e^{-\beta\mathcal{H}}\{0,1,0,1\}\longrightarrow e^{-\frac{U\beta}{4}}\mathrm{diag}\left(0,e^{\beta(U/2+\mu)},0,e^{2\mu\beta}\right)\\
n_\downarrow e^{-\beta\mathcal{H}} &= e^{-\beta\mathcal{H}}\{0,0,1,1\}\longrightarrow e^{-\frac{U\beta}{4}}\mathrm{diag}\left(0,0,e^{\beta(U/2+\mu)},e^{2\mu\beta}\right)\\
n_\uparrow n_\downarrow e^{-\beta\mathcal{H}} &= e^{-\beta\mathcal{H}}\{0,0,0,1\}\longrightarrow e^{-\frac{U\beta}{4}}\mathrm{diag}\left(0,0,0,e^{2\mu\beta}\right)
\end{aligned}$$

The traces of these operators are

$$\begin{aligned}
\mathrm{Tr}(\mathcal{H}e^{-\beta\mathcal{H}}) &= e^{-\frac{U\beta}{4}}\left(\frac{U}{4}+2(-\mu-\frac{U}{4})e^{\beta(U/2+\mu)}+(\frac{U}{4}-2\mu)e^{2\mu\beta}\right),\\
\mathrm{Tr}((n_\uparrow+n_\downarrow)e^{-\beta\mathcal{H}}) &= e^{-\frac{U\beta}{4}}\left(2e^{\beta(U/2+\mu)}+2e^{2\mu\beta}\right),\\
\mathrm{Tr}(n_\uparrow n_\downarrow e^{-\beta\mathcal{H}}) &= e^{-\frac{U\beta}{4}}e^{2\mu\beta}.
\end{aligned}$$

By the definition (1.2.2), the following physical observables $\mathcal{E}$ can be computed exactly:

1. The one-site density $\rho=\langle n_\uparrow\rangle+\langle n_\downarrow\rangle$ to measure the average occupation of each site:

$$\begin{aligned}
\rho &= \langle n_\uparrow\rangle+\langle n_\downarrow\rangle=\frac{\mathrm{Tr}\left((n_\uparrow+n_\downarrow)e^{-\beta\mathcal{H}}\right)}{\mathrm{Tr}(e^{-\beta\mathcal{H}})}\\
&= \frac{2e^{(\frac{U}{2}+\mu)\beta}+2e^{2\mu\beta}}{1+2e^{(\frac{U}{2}+\mu)\beta}+e^{2\mu\beta}}.
\end{aligned}$$

   In particular, when there is no chemical potential, i.e., $\mu=0$, then $\rho=1$. One refers to this as "half-filling" because the density is one-half the maximal possible value.

2. The one-site energy $E=\langle\mathcal{H}\rangle$:

$$\begin{aligned}
E &= \langle\mathcal{H}\rangle=\frac{\mathrm{Tr}(\mathcal{H}e^{-\beta\mathcal{H}})}{\mathrm{Tr}(Z)}\\
&= \frac{U}{4}-\frac{(2\mu+U)e^{(\frac{U}{2}+\mu)\beta}+2\mu e^{2\mu\beta}}{1+2e^{(\frac{U}{2}+\mu)\beta}+e^{2\mu\beta}}.
\end{aligned}$$

   In particular, when there is no chemical potential, i.e., $\mu=0$, then

$$E=\frac{U}{4}-\frac{U}{2(1+e^{-\frac{U\beta}{2}})}.$$

   Figure 1.1 shows the plot of E versus U and β.

3. The double occupancy $\langle n_\uparrow n_\downarrow\rangle$ is

$$\langle n_\uparrow n_\downarrow\rangle=\frac{\mathrm{Tr}(n_\uparrow n_\downarrow e^{-\beta\mathcal{H}})}{\mathrm{Tr}(Z)}=\frac{e^{2\mu\beta}}{1+2e^{(\frac{U}{2}+\mu)\beta}+e^{2\mu\beta}}.$$

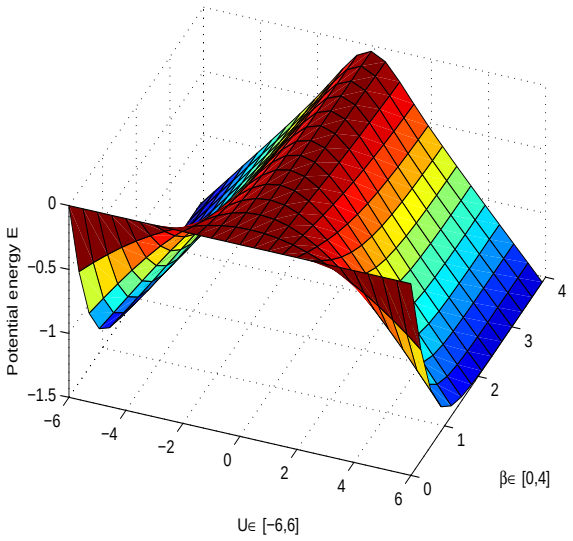

Figure 1.1: Potential energy E for $t = 0, \mu = 0$

In particular, when there is no chemical potential, i.e., $\mu = 0$,

$$\langle n_\uparrow n_\downarrow \rangle = \frac{1}{2(1 + e^{\frac{U}{2}\beta})}.$$

Note that as U or $\beta = 1/T$ increases, the double occupancy goes to zero.

1.2.2 Hubbard model without Coulomb interaction

When there is no Coulomb interaction, i.e., $U = 0$, the two spin spaces are independent of each other ($\mathcal{H}$ breaks into two separate pieces in which $\uparrow$ and $\downarrow$ terms never occur together). In this case we can consider each spin separately. If the spin is omitted, the Hamiltonian $\mathcal{H}$ becomes

$$\mathcal{H} = -t \sum_{\langle i,j \rangle} (c_i^\dagger c_j + c_j^\dagger c_i) - \mu \sum_i n_i.$$

It can be recast as a bilinear form:

$$\mathcal{H} = \vec{c}^\dagger (-tK - \mu I)\, \vec{c},$$

where K is a matrix to describe the hopping relationship $\langle i, j \rangle$, I is the identity matrix, and

$$\vec{c} = \begin{bmatrix} c_1 \\ c_2 \\ \vdots \\ c_N \end{bmatrix}, \quad \vec{c}^\dagger = [c_1^\dagger,\ c_2^\dagger,\ \cdots,\ c_N^\dagger].$$

For the one dimensional (1D) lattice of N_x sites, K is an $N_x \times N_x$ matrix given by

$$K = K_x = \begin{bmatrix} 0 & 1 & & 1 \\ 1 & 0 & 1 & \\ & \ddots & \ddots & \ddots \\ 1 & & 1 & 0 \end{bmatrix}.$$

The $(1, N_x)$ and $(N_x, 1)$ elements of K incorporate the so-called "periodic boundary conditions (PBCs)" in which sites 1 and N_x are connected by t. The use of PBC reduces finite size effects. For example, the energy on a finite lattice of length N with open boundary conditions (OBCs) differs from the value in the thermodynamic limit ($N \to \infty$) by a correction of order $1/N$ while with PBCs, the correction is order $1/N^2$. [1] The use of PBCs also makes the system translationally invariant. The density of electrons per site, and other similar quantities, will not depend on the site in question. With OBCs quantities will vary with the distance from the edges of the lattice.

For a two dimensional (2D) rectangle lattice of $N_x \times N_y$ sites, K is a $N_x N_y \times N_x N_y$ matrix given by

$$K = K_{xy} = I_y \otimes K_x + K_y \otimes I_x,$$

where I_x and I_y are identity matrices with dimensions N_x and N_y, respectively. $\otimes$ is the matrix Kronecker product.

The matrix K of 1D or 2D has the exact eigen-decomposition

$$K = F^T \Lambda F, \quad F^T F = I,$$

where $\Lambda = \mathrm{diag}(\lambda_k)$ is a diagonal eigenvalue matrix, see Lemma 2.3.1.

Let $\vec{\tilde{c}} = F\vec{c}$ and $\vec{\tilde{c}}^\dagger = (F\vec{c})^\dagger$, then the Hamiltonian $\mathcal{H}$ is diagonalized:

$$\mathcal{H} = \vec{\tilde{c}}^\dagger(-t\Lambda - \mu I)\vec{\tilde{c}} = \sum_k \epsilon_k \tilde{n}_k,$$

where $\epsilon_k \equiv -t\lambda_k - \mu$, and $\tilde{n}_k = \tilde{c}_k^\dagger \tilde{c}_k$. As we note in Remark 1.2.4, this transformation preserves the anticommutation relations, so $\tilde{c}_k$ still represents fermion operators.

Lemma 1.2.1 *If the operator $\mathcal{H}$ is in a quadratic form of fermion operators*

$$\mathcal{H} = c^\dagger H c,$$

where H is a Hermitian matrix. Then

$$\mathrm{Tr}(e^{-\beta\mathcal{H}}) = \prod_{k=1}^{N}(1 + e^{-\beta\lambda_k}),$$

where λ_k are the eigenvalues of H.

[1] A simple analogy is this: Consider numerical integration of $f(x)$ on an interval $a \le x \le b$. The only difference between the rectangle and trapezoidal rules is in their treatment of the boundary point contributions $f(a)$ and $f(b)$, yet the integration error changes from linear in the mesh size to quadratic.

PROOF. Since H is Hermitian matrix, there exists a unitary matrix Q such that

$$Q^* H Q = \Lambda = \mathrm{diag}(\lambda_k).$$

Let $\tilde{c} = Qc$ and $\tilde{n}_i = \tilde{c}_i^\dagger \tilde{c}_i$, then we have

$$\mathcal{H} = \tilde{c}^\dagger \Lambda \tilde{c} = \sum_{i=1}^{N} \lambda_i \tilde{n}_i.$$

Note that the $\tilde{n}_i$ are independent, then

$$\mathrm{Tr}(e^{-\beta\mathcal{H}}) = \mathrm{Tr}\left(\prod_{i=1}^{N} e^{-\beta\lambda_i \tilde{n}_i}\right) = \prod_{i=1}^{N}(1 + e^{-\beta\lambda_i}), \tag{1.2.8}$$

where the last equality can be obtained by an induction argument. ∎

Note that the trace is independent of the basis functions. If we choose the eigen-functions of the operator $\tilde{n}_k$ as the basis functions, then by Lemma 1.2.1, the partition function $\mathcal{Z}$ is given by

$$Z = \prod_k (1 + e^{\beta\epsilon_k}).$$

Consequently, we have the exact expressions for the following physical observables $\mathcal{E}$:

1. the density ρ, the average occupation of each site:

$$\rho = \langle n \rangle = \langle \tilde{n} \rangle = \frac{1}{N} \sum_{k=1}^{N} \langle \tilde{n}_{k\uparrow} + \tilde{n}_{k\downarrow} \rangle = \sum_k (1 + e^{\beta\epsilon_k})^{-1},$$

2. the energy E:

$$E = \langle \mathcal{H} \rangle = \frac{1}{N} \sum_k \frac{\epsilon_k + \mu}{e^{\beta\epsilon_k} + 1}. \tag{1.2.9}$$

Remark **1.2.5** *It can be shown that the operators $\tilde{c}_k$ obey the same anticommutation relations as the original operators c_i. Hence they too appropriately describe electrons. Indeed, the original operators create and destroy particles on particular spatial sites i while the new ones create and destroy with particular momenta k. Either set is appropriate to use, however, the interaction term in the Hubbard model is fairly complex when written in momentum space.*

For the sake of completeness, let us write down the expression for the Green's function. This quantity plays a key role in the discussion of the matrices arising in the simulation which follows

$$G_{\ell,n} = \langle c_\ell c_n^\dagger \rangle = \frac{1}{N} \sum_k e^{ik\cdot(n-\ell)}(1 - f_k), \tag{1.2.10}$$

where $f_k = 1/[1 + e^{\beta(\epsilon_k - \mu)}]$. Notice that G is a function of the difference $n - \ell$. This is a consequence of the fact that the Hamiltonian is translationally invariant, that is, with PBCs, there is no special site which is singled out as the origin of the lattice. All sites are equivalent.

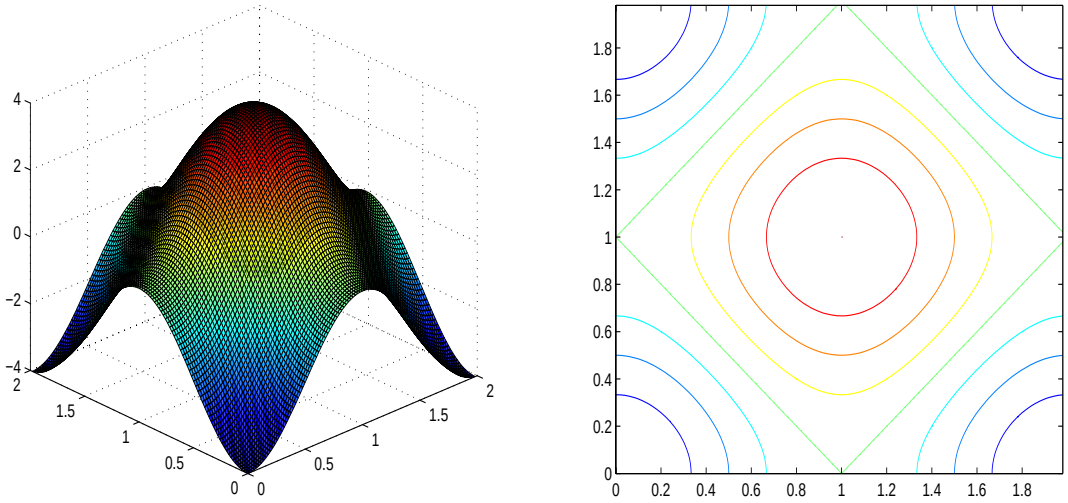

Figure 1.2: Left: ϵ_k for $U = 0$ and $\mu = 0$. Right: the contour plot of ϵ_k

At $T = 0$ ($\beta = \infty$), the contours in the right side of Figure 1.2 separate the k values where the states are occupied $f_k = 1$ (inside the contour) from those where the states are empty $f_k = 0$ (outside the contour). The contour is often referred to as the "Fermi surface". There is actually a lot of interesting physics which follows from the geometry of the contour plot of ϵ_k. For example, one notes that the vector (π, π) connects large regions of the contour in the case when $\rho = 1$ and the contour is the rotated square connecting the points $(\pi, 0), (0, \pi), (-\pi, 0)$, and $(0, -\pi)$. One refers to this phenomenon as "nesting" and to (π, π) as the "nesting wave vector". Because the Fermi surface describes the location where the occupation changes from 0 to 1, the electrons are most active there. If there is a wave vector k which connects big expanses of these active regions, special order is likely to occur with that wave vector. Thus the contour plot of ϵ_k is one way of understanding the tendency of the Hubbard model to have *antiferromagnetic* order (magnetic order at $k = (\pi, \pi)$ for half-filling.)

1.3 Determinant QMC

In this section, we develop a computable approximation of the distribution operator $\mathcal{P}$ in (1.2.3) by using a discrete Hubbard-Stratonovich transformation, and then we derive a so-called determinant QMC (DQMC) to generate samples that follow the distribution. For simplicity, we will consider the chemical potential $\mu = 0$ which corresponds to the important half-filled-band case. It turns out that many of the most interesting phenomena of the Hubbard model, like magnetic ordering and insulating-metal transition, occur at half filling.

1.3.1 Computable approximation of distribution operator $\mathcal{P}$

The gist of a computable approximation of the distribution operator $\mathcal{P}$ defined in (1.2.3) is on the approximation of the partition function $\mathcal{Z}$. Since the operators $\mathcal{H}_K$ and $\mathcal{H}_V$ do not commute, we apply the Suzuki-Trotter decomposition to approximate $\mathcal{Z}$. Specifically, divide β into L smaller subintervals $\tau = \frac{\beta}{L}$, then $\mathcal{Z}$ is approximated by

$$\begin{aligned}\mathcal{Z} &= \mathrm{Tr}\left(e^{-\beta\mathcal{H}}\right)\\ &= \mathrm{Tr}\left(\prod_{\ell=1}^{L} e^{-\tau\mathcal{H}}\right)\\ &= \mathrm{Tr}\left(\prod_{\ell=1}^{L} e^{-\tau\mathcal{H}_K} e^{-\tau\mathcal{H}_V}\right) + O(\tau^2). \end{aligned} \tag{1.3.11}$$

Note that $e^{-\tau\mathcal{H}_K}$ is quadratic in the fermion operators and the operators for the spin-up and spin-down operators are independent. Therefore, it can be recast as

$$e^{-\tau\mathcal{H}_K} = e^{-\tau H_{K_+}} e^{-\tau H_{K_-}},$$

where the operators $\mathcal{H}_{K_+}$ and $\mathcal{H}_{K_-}$ correspond to kinetic energy with spin-up and spin-down respectively, and are of the forms

$$\begin{aligned}\mathcal{H}_{K_+} &= t\,\vec{c}_\uparrow^{\,\dagger} K \vec{c}_\uparrow,\\ \mathcal{H}_{K_-} &= t\,\vec{c}_\downarrow^{\,\dagger} K \vec{c}_\downarrow.\end{aligned}$$

On the other hand, the potential energy $e^{-\tau\mathcal{H}_V}$ is quartic in the fermion operators. We now try to recast it in a quadratic form. First, note that the number operators n_i are independent on different sites, we have

$$e^{-\tau\mathcal{H}_V} = e^{-U\tau\sum_{i=1}^{N}(n_{i+}-\frac{1}{2})(n_{i-}-\frac{1}{2})} = \prod_{i=1}^{N} e^{-U\tau(n_{i+}-\frac{1}{2})(n_{i-}-\frac{1}{2})}.$$

For treating the term $e^{-U\tau(n_{i+}-\frac{1}{2})(n_{i-}-\frac{1}{2})}$, we use the following so-called discrete Hubbard-Stratonovich transformation. It replaces the interaction (potential energy) quartic terms $n_{i+}n_{i-}$ by quadratic ones $n_{i+} - n_{i-}$.

Lemma 1.3.1 *(Discrete Hubbard-Stratonovich transformation, [2, 4]). If $U > 0$, then*

$$e^{-U\tau(n_{i+}-\frac{1}{2})(n_{i-}-\frac{1}{2})} = C_1 \sum_{h_i=\pm 1} e^{\nu h_i(n_{i+}-n_{i-})}, \tag{1.3.12}$$

where $C_1 = \frac{1}{2}e^{-\frac{U\tau}{4}}$ and $\cosh\nu = e^{\frac{U\tau}{2}}$.

Proof. On every site i, the particles have four possible states: $|\cdot\rangle$, $|\uparrow\rangle$, $|\downarrow\rangle$ and $|\uparrow\downarrow\rangle$. The following table lists the actions of the operators $(n_{i+} - \frac{1}{2})(n_{i-} - \frac{1}{2})$ and $(n_{i+} - n_{i-})$.

	$(n_{i+}-\frac{1}{2})(n_{i-}-\frac{1}{2})$	$(n_{i+}-n_{i-})$
$\|\cdot\rangle$	$\frac{1}{4}\|\cdot\rangle$	$0\ \|\cdot\rangle$
$\|\uparrow\rangle$	$-\frac{1}{4}\|\uparrow\rangle$	$\|\uparrow\rangle$
$\|\downarrow\rangle$	$-\frac{1}{4}\|\downarrow\rangle$	$\|\downarrow\rangle$
$\|\uparrow\downarrow\rangle$	$\frac{1}{4}\|\uparrow\downarrow\rangle$	$0\ \|\uparrow\downarrow\rangle$

For the operator $e^{-U\tau(n_{i+}-\frac{1}{2})(n_{i-}-\frac{1}{2})}$:

$$e^{-U\tau(n_{i+}-\frac{1}{2})(n_{i-}-\frac{1}{2})}\psi = e^{-\frac{U\tau}{4}}\psi \quad \text{if} \quad \psi = |\cdot\rangle \text{ or } |\uparrow\downarrow\rangle,$$

and

$$e^{-U\tau(n_{i+}-\frac{1}{2})(n_{i-}-\frac{1}{2})}\psi = e^{\frac{U\tau}{4}}\psi \quad \text{if} \quad \psi = |\uparrow\rangle \text{ or } |\downarrow\rangle.$$

On the other hand, for the operator $C_1\sum_{h_i=\pm 1} e^{\nu h_i(n_{i+}-n_{i-})}$:

$$C_1\sum_{h_i=\pm 1} e^{\nu h_i(n_{i+}-n_{i-})}\psi = e^{-\frac{U\tau}{4}}\psi \quad \text{and} \quad \psi = |\cdot\rangle \text{ or } |\uparrow\downarrow\rangle,$$

and

$$C_1\sum_{h_i=\pm 1} e^{\nu h_i(n_{i+}-n_{i-})}\psi = \frac{1}{2}e^{-\frac{U\tau}{4}}(e^{\nu}+e^{-\nu})\psi \quad \text{if} \quad \psi = |\uparrow\rangle \text{ or } |\downarrow\rangle.$$

Therefore if we let

$$\cosh\nu = \frac{e^{\nu}+e^{-\nu}}{2} = e^{\frac{U\tau}{2}},$$

then the discrete Hubbard-Stratonovich transformation (1.3.12) holds. □

Remark **1.3.1**

- *Note that in the proof, U is required to be positive, otherwise no real number ν exists such that* $\cosh\nu = e^{\frac{U\tau}{2}}$.
- *For $U<0$, the Hubbard model is called the attractive Hubbard model. A similar discrete Hubbard-stratonovich transformation also exists, see [5, 6].*
- *See [12, 16] for other kind of transformations treating the quartic term.*

Let us continue to reformulate the term $e^{-\tau\mathcal{H}_V}$. By the following discrete Hubbard-Stratonovich transformation (1.3.12), we have[2]

$$e^{-\tau\mathcal{H}_V} = \prod_{i=1}^{N}\left(C_1\sum_{h_i=\pm 1} e^{\nu h_i(n_{i+}-n_{i-})}\right). \tag{1.3.13}$$

$\{h_i\}$ are so-called auxiliary Hubbard-Stratonovich variables, one for each spatial site. The collection of all these variables is called the "Hubbard-Stratonovich field" or "configurations".

[2]Here we switch the notation: $n_{i+}=n_{i\uparrow}$ and $n_{i-}=n_{i\downarrow}$.

For the sake of simplicity, let us consider the case $N = 2$ for the expression (1.3.13):

$$\begin{aligned} e^{-\tau\mathcal{H}_V} &= (C_1)^2 \left(\sum_{h_i=\pm 1} e^{\nu h_i (n_{1+}-n_{1-})} \right) \left(\sum_{h_i=\pm 1} e^{\nu h_i (n_{2+}-n_{2-})} \right) \\ &= (C_1)^2 \sum_{h_i=\pm 1} e^{\sum_{i=1}^{2} \nu h_i (n_{i+}-n_{i-})} \\ &\equiv (C_1)^2 \mathrm{Tr}_h e^{\sum_{i=1}^{2} \nu h_i (n_{i+}-n_{i-})}, \end{aligned}$$

where the new notation Tr_h represents the sum for $h_i = 1, -1$.

In general, we have

$$\begin{aligned} e^{-\tau\mathcal{H}_V} &= (C_1)^N \mathrm{Tr}_h e^{\sum_{i=1}^{N} \nu h_i (n_{i+}-n_{i-})} \\ &= (C_1)^N \mathrm{Tr}_h \left(e^{\sum_{i=1}^{N} \nu h_i n_{i+}} e^{\sum_{i=1}^{N} -\nu h_i n_{i-}} \right) \\ &\equiv (C_1)^N \mathrm{Tr}_h (e^{\mathcal{H}_{V_+}} e^{\mathcal{H}_{V_-}}), \end{aligned} \tag{1.3.14}$$

where $\mathcal{H}_{V_+}$ and $\mathcal{H}_{V_-}$ correspond to spin-up and spin-down, respectively, and are of the forms

$$\begin{aligned} \mathcal{H}_{V_+} &= \sum_{i=1}^{N} \nu h_i n_{i+} = \vec{c}_+^{\,\dagger} V(h) \vec{c}_+, \\ \mathcal{H}_{V_-} &= -\sum_{i=1}^{N} \nu h_i n_{i-} = -\vec{c}_-^{\,\dagger} V(h) \vec{c}_-, \end{aligned}$$

where $V(h)$ is a diagonal matrix $V(h) = \nu \cdot \mathrm{diag}(\, h_1, h_2, \ldots, h_N \,)$.

Taking into the account of the discretization of the inverse temperature β partitioned into L "imaginary-time" slices, $L = \beta/\tau$, the Hubbard-Stratonovich variables h_i are changed to have two subindices $h_{\ell,i}$, where i is for the spatial site and ℓ is for the time slice. Correspondingly, the index ℓ is also introduced for the diagonal matrix V and operators $\mathcal{H}_{V_\sigma}$, i.e.,

$$h_i \longrightarrow h_{\ell,i}, \qquad V \longrightarrow V_\ell, \qquad \mathcal{H}_{V_\sigma} \longrightarrow \mathcal{H}_{V_\sigma}^{\ell}.$$

Subsequently, by applying the Suzuki–Trotter approximation (1.3.11) and the expression (1.3.14) and interchanging the traces, the partition function $\mathcal{Z}$ can be approximated by

$$\mathcal{Z} = (C_1)^{NL} \mathrm{Tr}_h \mathrm{Tr} \left(\prod_{\ell=1}^{L} e^{-\tau\mathcal{H}_{K_+}} e^{\mathcal{H}_{V_+}^{\ell}} \right) \left(\prod_{\ell=1}^{L} e^{-\tau\mathcal{H}_{K_-}} e^{\mathcal{H}_{V_-}^{\ell}} \right). \tag{1.3.15}$$

where for $\sigma = \pm$,

$$\begin{aligned} \mathcal{H}_{K_\sigma} &= t\, \vec{c}_\sigma^{\,\dagger} K \vec{c}_\sigma, \\ \mathcal{H}_{V_\sigma}^{\ell} &= \sigma \sum_{i=1}^{N} \nu h_{\ell,i} n_{i+} = \sigma \vec{c}_\sigma^{\,\dagger} V_\ell(h_\ell) \vec{c}_\sigma \end{aligned}$$

and $V_\ell(h_\ell)$ is a diagonal matrix $V_\ell(h_\ell) = \nu \cdot \mathrm{diag}(\, h_{\ell,1}, h_{\ell,2}, \ldots, h_{\ell,N}\,)$.

Note that all operators $\mathcal{H}_{K_+}$, $\mathcal{H}_{K_-}$, $\mathcal{H}^\ell_{V+}$ and $\mathcal{H}^\ell_{V-}$ are quadratic in the fermion operators. We now turn to an identity, referred to as *Hirsch's argument* [4][3]:

Hirsch's argument. If operators $\mathcal{H}_\ell$ are in the quadratic form of fermion operators

$$\mathcal{H}_\ell = \sum_{i,j} c_i^\dagger (H_\ell)_{ij} c_j,$$

where H_ℓ are matrices of real numbers. Then[4],

$$\mathrm{Tr}(e^{-\mathcal{H}_1} e^{-\mathcal{H}_2} \cdots e^{-\mathcal{H}_L}) = \det(I + e^{-H_L} e^{-H_{L-1}} \cdots e^{-H_1}). \tag{1.3.16}$$

By using the identity (1.3.16), the partition function $\mathcal{Z}$ described in (1.3.15) is turned into the following computable form

$$Z_h = (C_1)^{NL} \mathrm{Tr}_h \det[M_+(h)] \det[M_-(h)], \tag{1.3.17}$$

where for $\sigma = \pm$ and $h = (h_1, h_2, \ldots, h_L)$,

$$M_\sigma(h) = I + B_{L,\sigma}(h_L) B_{L-1,\sigma}(h_{L-1}) \cdots B_{1,\sigma}(h_1), \tag{1.3.18}$$

$B_{\ell,\sigma}(h_\ell)$ are $N \times N$ matrices defined as

$$B_{\ell,\sigma}(h_\ell) = e^{-t\tau K} e^{\sigma V_\ell(h_\ell)},$$

which correspond to operators $e^{-\tau \mathcal{H}_K} e^{-\tau \mathcal{H}^\ell_{V\sigma}}$.

In summary, upto a constant, we have a computable approximation of the distribution operator $\mathcal{P}$:

$$P(h) = \frac{1}{Z_h} \det[M_+(h)] \det[M_-(h)], \tag{1.3.19}$$

which is referred to as a probability distribution function (pdf).

Remark **1.3.2** *When $U = 0$, then $\nu = 0$ and $M_\sigma(h)$ is a constant matrix which does not depend on the configuration h. The approximation by the Trotter decomposition is exact.*

Remark **1.3.3** *It is a rather amazing thing that a quantum problem can be re-written as a classical one. The price for this is that the classical problem is in one higher dimension than the original quantum one: the degrees of freedom in the quantum problem c_i had a single spatial index i while the Hubbard Stratonovich variables which replace them have an additional 'imaginary time' index ℓ. This mapping is by no means restricted to the Hubbard Hamiltonian, but is generally true for all quantum mechanics problems.*

[3] We are not able to provide a rigorous full proof for this important identity. For the special case $L = 1$, the result has been proven in Lemma 1.2.1.

[4] Note that while "Tr" is over the quantum mechanical Hilbert space whose dimension is 4^N, and the "det" is a usual determinant of a $N \times N$ matrix. By Pauli exclusion principle, there are 4 possible states in every lattice: no electron, one electron with spin-up, one electron with spin-down and two electron with different spin.

1.3.2 Generating states in determinant QMC

At this stage, the computational task becomes a classical Monte Carlo problem: compute random variables h that follow the probability distribution function $P(h)$, i.e.,

$$h \sim P(h). \tag{1.3.20}$$

The random variables h are referred to as the Hubbard-Stratonovich variables or configurations. The dimension of the configuration sample space $\{h\}$ is 2^{NL}. For an efficient Monte Carlo procedure there are two central questions:

1. How to move to a new configuration h' from h?

   A simple strategy is to flip only at one selected site (ℓ, i)

   $$h'_{\ell,i} = -h_{\ell,i},$$

   and leave the rest components of h unchanged.

2. How to ensure that the accepted sample configuration h follows the desired distribution $P(h)$?

   This is done by the Metropolis-Hasting algorithm, for example, see [9, p.111].

Combining the answers of these two questions, we have the following so-called determinant QMC (DQMC) simulation, first presented in [2].

DQMC:

1. initialize $h = (h_{\ell,i}) = (\pm 1)$
2. MC loop (= warmup + measurement steps)
   (a) (ℓ, i) loop:
      i. set $(\ell, i) = (1, 1)$
      ii. propose a new configuration h' by spin-flipping at (ℓ, i): $h'_{\ell,i} = -h_{\ell,i}$
      iii. compute the Metropolis ratio

$$r_{\ell,i} = \frac{\det[M_+(h')]\det[M_-(h')]}{\det[M_+(h)]\det[M_-(h)]}$$

      iv. accept or reject: generate a random number $r \sim \text{Uniform}[0, 1]$ and update

$$h = \begin{cases} h', & \text{if } r \leq \min\{1, r_{\ell,i}\} \\ h, & \text{otherwise.} \end{cases}$$

      v. update Green's function $G(h)(= M(h)^{-1})$, if "accepted"
      vi. go to the next site (ℓ, i), where
      - If $\ell = L$ and $i = N$, then $\ell := 1, i = 1$;
      - If $\ell < L$ and $i = N$, then $\ell := \ell + 1, i = 1$;
      - If $i < N$, then $\ell := \ell$, $i := i + 1$.

   (b) after the warmup steps, perform physical measurements, see section 1.3.3

Note that the simple one-site update at the inner loop leads to a simple rank-one updating in one of the block matrices $B_{\ell,\sigma}(h_\ell)$. Based on this observation, one can efficiently compute the Matropolis $r_{\ell,i}$ and update the Green's function $G_\sigma(h) = (M_\sigma(h))^{-1}$ for physical measurements, see Appendix A for detail.

1.3.3 Physical measurements

How is the physics extracted from QMC simulations? Two of the most elementary physical observables of interest are the *density* and *kinetic energy*, which can be obtained from the single-particle Green's function,

$$\begin{aligned} G^\sigma_{ij} &= \langle c_{i\sigma} c^\dagger_{j\sigma} \rangle \\ &= (M_\sigma(h))^{-1}_{ij} \\ &= [I + B_{L,\sigma}(h_L) B_{L-1,\sigma}(h_{L-1}) \cdots B_{1,\sigma}(h_1)]^{-1}_{ij} . \end{aligned}$$

The density of electrons of spin σ on site i is

$$\rho_{i,\sigma} = \langle n_{i,\sigma} \rangle = \langle c^\dagger_{i,\sigma} c_{i,\sigma} \rangle = 1 - \langle c_{i,\sigma} c^\dagger_{i,\sigma} \rangle = 1 - G^\sigma_{ii},$$

where the third identity arises from the use of the anticommutation relations in interchanging the order of creation and destruction operators.

The Hubbard Hamiltonian is translationally invariant, so one expects $\rho_{i,\sigma}$ to be independent of spatial site i. Likewise, up and down spin species are equivalent. Thus to reduce the statistical errors, one usually averages all the values and have the code report back

$$\rho = \frac{1}{2N} \sum_\sigma \sum_{i=1}^{N} \rho_{i,\sigma}.$$

We will not emphasize this point further, but such averaging is useful for most observables. [5] As is true in any classical or quantum monte carlo, these expectation values are also averaged over the sequence of Hubbard-Stratonovich configurations generated in the simulation.

The kinetic energy is obtained from the Green's function for pairs of sites i, j which are near neighbors,

$$\langle \mathcal{H}_K \rangle = -t \, \langle \sum_{\langle i,j \rangle, \sigma} (c^\dagger_{i\sigma} c_{j\sigma} + c^\dagger_{j\sigma} c_{i\sigma}) \rangle = +t \sum_{\langle i,j \rangle, \sigma} (G^\sigma_{ij} + G^\sigma_{ji}).$$

An extra minus sign arose from interchanging the fermion operator order so that the creation operator was at the right.

Extended physical measurements. Interesting types of magnetic, charge, and superconducting order, and associated phase transitions, are determined by looking at correlation functions of the form:

$$c(l) = \langle \mathcal{O}_{i+l} \mathcal{O}^\dagger_i \rangle - \langle \mathcal{O}_{i+l} \rangle \, \langle \mathcal{O}^\dagger_i \rangle \tag{1.3.21}$$

where, for example,

[5] There are some situations where translation invariance is broken, for example if randomness is included in the Hamiltonian.

- for spin order in z direction (magnetism):

$$\mathcal{O}_i = n_{i,\uparrow} - n_{i,\downarrow} \quad \mathcal{O}_i^\dagger = n_{i,\uparrow} - n_{i,\downarrow}$$

- for spin order in x/y direction (magnetism):

$$\mathcal{O}_i = c_{i,\downarrow}^\dagger c_{i,\uparrow} \quad \mathcal{O}_i^\dagger = c_{i,\uparrow}^\dagger c_{i,\downarrow}$$

- for charge order:

$$\mathcal{O}_i = (n_{i,\uparrow} + n_{i,\downarrow}) \quad \mathcal{O}_i^\dagger = (n_{i,\uparrow} + n_{i,\downarrow})$$

- for pair order (superconductivity):

$$\mathcal{O}_i = c_{i,\downarrow} c_{i,\uparrow} \quad \mathcal{O}_i^\dagger = c_{i,\uparrow}^\dagger c_{i,\downarrow}^\dagger$$

In words, what such correlation functions probe is the relationship between spin, charge, pairing on an initial site i with that on a site $i+l$ separated by a distance l. It is plausible that at high temperatures where there is a lot of random thermal vibration, the values of $\mathcal{O}_i^\dagger$ and $\mathcal{O}_{i+l}$ will not 'know about' each other for large l. In such a case, the expectation value $\langle \mathcal{O}_{i+l} \mathcal{O}_i^\dagger \rangle$ factorizes to $\langle \mathcal{O}_{i+l} \rangle \langle \mathcal{O}_i^\dagger \rangle$ and $c(l)$ vanishes. The more precise statement is that at high temperatures $c(l)$ decays exponentially, $c(l) \propto e^{-l/\xi}$. The quantity ξ is called the "correlation length". On the other hand, at low temperatures $c(l) \propto \alpha^2$, a nonzero value, as $l \to \infty$. The quantity α is called the 'order parameter'. [6]

As one can well imagine from this description, one needs to be very careful in analyzing data on finite lattices if the $l \to \infty$ behavior is what is crucial to determining the physics. The techniques of 'finite size scaling' provide methods for accomplishing this.

How are these correlation functions actually evaluated? As commented above in describing measurements of the density and kinetic energy, expectation values of two fermion operators are simply expressed in terms of the Greens function $G = M^{-1}$. The general rule for expectation values of more than two fermion creation and destruction operators is that they reduce to products of expectation values of pairs of creation and destruction operators, the famous 'Wick's Theorem' of many body physics. For example, for spin order in the x/y direction,

$$\langle c(l) \rangle = \langle c_{i+l,\downarrow}^\dagger c_{i+l,\uparrow} c_{i,\uparrow}^\dagger c_{i,\downarrow} \rangle = G_{i+l,i}^\uparrow \, G_{i,i+l}^\downarrow. \tag{1.3.22}$$

Similarly, for superconducting order,

$$\langle c(l) \rangle = \langle c_{i+l,\downarrow} c_{i+l,\uparrow} c_{i,\uparrow}^\dagger c_{i,\downarrow}^\dagger \rangle = G_{i+l,i}^\uparrow \, G_{i+l,i}^\downarrow. \tag{1.3.23}$$

We conclude with two comments. First, it is useful to look at correlation functions where the operators $\mathcal{O}_{i+l}$ and $\mathcal{O}_i^\dagger$ are separated in imaginary time as well as in space. We will come to this point when we discuss measurements in the hybrid QMC algorithm. Second, one often considers the Fourier transform of the real space correlation function $S(q) = \sum_l e^{iql} \, c(l)$. This quantity is often referred to as the 'structure factor', and is important because it is in fact the quantity measured by experimentalists. (For example, the scattering rate of a neutron off the electron spins in a crystal is proportional to $S(q)$ where q is the change in momentum of the neutron and the $c(l)$ under consideration is the spin correlation function.)

[6] It is interesting to note what happens right at the critical point T_c separating the high temperature disordered phase from the low temperature ordered one. In what are termed 'second order' phase transitions, the correlation length diverges $\xi \propto 1/(T - T_c)^\nu$. Right at T_c the correlation function decays as a power law, $c(l) \propto 1/l^\eta$, a behavior intermediate between its high temperature exponential decay and its low temperature nonzero value.

1.4 Hybrid QMC

The procedure summarized in section 1.3.2 is the one used in most DQMC codes today. Many interesting physical results have been obtained with it. However, it has a crucial limitation. At the heart of the procedure is the need to compute determinants and inverses of matrices which have a dimension the spatial size of the system, N. Thus the algorithm scales as N^3. In practice, this means simulations are limited to a few hundred sites. In order to circumvent this bottleneck and develop an algorithm which potentially scales linearly with N, we can reformulate our problem as the following:

1. replace the discrete Hubbard-Stratonovich field by a continuous one;
2. express the determinant of the dense $N \times N$ matrices $M_\sigma(h)$ as Gaussian integrals over NL-dimensional sparse matrices.

We shall now describe each of these steps in detail.

1.4.1 Computable approximation of the distribution operator $\mathcal{P}$

Instead of using discrete Hubbard-Stratonovich transformation as described in section 1.3.1, one can use a continuous Hubbard-Stratonovich transformation to derive a computable approximation of the distribution operator $\mathcal{P}$. First, recall the Stratonovich identity:

$$e^{\frac{1}{2}a^2} = \frac{1}{\sqrt{2\pi}} \int_{-\infty}^{\infty} e^{-\frac{1}{2}x^2 - xa} dx$$

for any scalar $a > 0$.

Lemma 1.4.1 *(Continuous Hubbard-Stratonovich transformation) For $U > 0$, we have*

$$e^{-U\tau(n_{i+}-\frac{1}{2})(n_{i-}-\frac{1}{2})} = C_2 \int_{-\infty}^{\infty} e^{-\tau[x^2+(2U)^{\frac{1}{2}}x(n_{i+}-n_{i-})]} dx, \tag{1.4.24}$$

where $C_2 = (\tau^{\frac{1}{2}} e^{-\frac{U\tau}{4}})/\pi^{\frac{1}{2}}$.

Proof. It is easy to verify that

$$(n_{i+} - \frac{1}{2})(n_{i-} - \frac{1}{2}) = -\frac{1}{2}(n_{i+} - n_{i-})^2 + \frac{1}{4}.$$

Note that $(n_{i+} - n_{i-})^2$ and $n_{i+} - n_{i-}$ can be diagonalized based on the eigen-states of the operators $n_{i\sigma}$, then the Stratonovich identity holds if we replace the scalar α by the operator $n_{i+} - n_{i-}$:

$$e^{\frac{U\tau}{2}(n_{i+}-n_{i-})^2} = \frac{1}{\sqrt{2\pi}} \int_{-\infty}^{\infty} e^{-\frac{1}{2}x^2 - (U\tau)^{\frac{1}{2}}(n_{i+}-n_{i-})x} dx.$$

Let $x' = \frac{x}{\sqrt{2\tau}}$, we have

$$e^{\frac{U\tau}{2}(n_{i+}-n_{i-})^2} = \frac{\sqrt{\tau}}{\sqrt{\pi}} \int_{-\infty}^{\infty} e^{-\tau(x^2+(2U)^{\frac{1}{2}}(n_{i+}-n_{i-})x)} dx.$$

Combining the above equations, we obtain the identity (1.4.24). □

Returning to the approximation of the partition function $\mathcal{Z}$ by the Suzuki-Trotter decomposition (1.3.11), by the continuous Hubbard-Stratonovich identity (1.4.24), we have

$$\begin{aligned} e^{-\tau\mathcal{H}_V^\ell} &= (C_2)^N \int_{-\infty}^{+\infty} e^{-\tau\sum_i x_{\ell,i}^2} e^{\tau\sum_i (2U)^{\frac{1}{2}} x_{\ell,i} n_{i+}} e^{-\tau\sum_i (2U)^{\frac{1}{2}} x_{\ell,i} n_{i-}} dx_{\ell,i} \\ &\equiv (C_2)^N \int [\delta x] e^{-S_B(x)} e^{\tau\mathcal{H}_{V_+}^\ell} e^{\tau\mathcal{H}_{V_-}^\ell}, \end{aligned}$$

where

$$\begin{aligned} S_B(x) &= \tau\sum_{\ell,i} x_{\ell,i}^2, \\ \mathcal{H}_{V_+}^\ell &= \sum_i (2U)^{\frac{1}{2}} x_{\ell,i} n_{i+} = \vec{c}_+^{\,\dagger} V_\ell(x_\ell)\vec{c}_+, \\ \mathcal{H}_{V_-}^\ell &= -\sum_i (2U)^{\frac{1}{2}} x_{\ell,i} n_{i-} = -\vec{c}_-^{\,\dagger} V_\ell(x_\ell)\vec{c}_-, \end{aligned}$$

and $V_\ell(x_\ell)$ is a diagonal matrix,

$$V_\ell(x_\ell) = (2U)^{\frac{1}{2}} \mathrm{diag}(x_{\ell,1}, x_{\ell,2}, \ldots, x_{\ell,N}).$$

By an analogous argument as in section 1.3.1, we have the following approximation of the partition function $\mathcal{Z}$:

$$\begin{aligned} \mathcal{Z} &= \mathrm{Tr}\left(\prod_{\ell=1}^L e^{-\tau\mathcal{H}_K} e^{-\tau\mathcal{H}_V}\right) \\ &= (C_2)^{NL} \int [\delta x] e^{-S_B(x)} \mathrm{Tr}\left(\prod_{\ell=1}^L e^{-\tau\mathcal{H}_{K_+}} e^{\tau\mathcal{H}_{V+}^\ell}\right) \mathrm{Tr}\left(\prod_{\ell=1}^L e^{-\tau\mathcal{H}_{K_-}} e^{\tau\mathcal{H}_{V-}^\ell}\right). \end{aligned}$$

Note that all the operators $e^{-\tau\mathcal{H}_K^\ell}$, $e^{-\tau\mathcal{H}_{V+}^\ell}$ and $e^{-\tau\mathcal{H}_{V-}^\ell}$ are quadratic in the fermion operators. Then by the Hirsch's argument (1.3.16), we derive the following expression for calculating the partition function $\mathcal{Z}$:

$$\begin{aligned} Z_x &= (C_2)^{NL} \int [\delta x] e^{-S_B(x)} \det\left(I + \prod_{\ell=1}^L e^{t\tau K} e^{\tau V_l(x_\ell)}\right) \det\left(I + \prod_{\ell=1}^L e^{t\tau K} e^{-\tau V_\ell(x_\ell)}\right) \\ &= (C_2)^{NL} \int [\delta x] e^{-S_B(x)} \det[M_+(x)] \det[M_-(x)], \end{aligned} \tag{1.4.25}$$

where for $\sigma = \pm$,

$$M_\sigma(x) = I + B_{L,\sigma}(x_L) B_{L-1,\sigma}(x_{L-1}) \cdots B_{1,\sigma}(x_1), \tag{1.4.26}$$

and

$$B_{\ell,\sigma}(x_\ell) = e^{t\tau K} e^{\sigma\tau V_\ell(x_\ell)}. \tag{1.4.27}$$

By a so-called particle-hole transformation (see Appendix B), we have

$$\det[M_-(x)] = e^{-\tau(2U)^{\frac{1}{2}}\sum_{\ell,i} x_{\ell,i}} \det[M_+(x)]. \tag{1.4.28}$$

Therefore, the integrand of Z_x in (1.4.25) is positive definite[7]

Consequently, up to a constant, a computable approximation of the distribution operator $\mathcal{P}$ is given by

$$P(x) = \frac{1}{Z_x} e^{-S_B(x)} \det[M_+(x)] \det[M_-(x)]. \tag{1.4.29}$$

$P(x)$ is referred to as a probability distribution function (pdf).

1.4.2 Hybrid QMC

The computational task becomes how to compute random variables x that follow the probability distribution function $P(x)$:

$$x \sim P(x), \tag{1.4.30}$$

where x is referred to as the configurations, or a continue Hubbard-Stratonovich variable.

To develop an efficient Monte Carlo method for (1.4.30), we reformulate the pdf $P(x)$. First, let us recall the following two facts:

1. Let $M_\sigma(x)$ denote a $L \times L$ block matrix[8]

$$\begin{aligned} M_\sigma(x) &= \begin{bmatrix} I & & & & & B_{1,\sigma}(x_1) \\ -B_{2,\sigma}(x_2) & I & & & & \\ & -B_{3,\sigma}(x_3) & I & & & \\ & & \ddots & \ddots & & \\ & & & -B_{L,\sigma}(x_L) & I & \end{bmatrix} \qquad (1.4.31) \\ &\equiv I - K_{[L]} V_{[L]}(x) \Pi, \qquad (1.4.32) \end{aligned}$$

   where $B_{\ell,\sigma}(x_\ell)$ are $N \times N$ matrices as defined in (1.4.27).

$$\begin{aligned} K_{[L]} &= \mathrm{diag}(e^{t\tau K}, e^{t\tau K}, \ldots, e^{t\tau K}), \\ V_{[L]}(x) &= \mathrm{diag}(e^{-\sigma\tau V_1(x_1)}, e^{-\sigma\tau V_2(x_2)}, \ldots, e^{-\sigma\tau V_L}(x_L)) \end{aligned}$$

   and

$$\Pi = \begin{bmatrix} 0 & & & -I \\ I & 0 & & \\ & \ddots & \ddots & \\ & & I & 0 \end{bmatrix}.$$

[7]Note that we assume that $\mu = 0$ (half-filling case). Otherwise, there exists "sign problem": $P(x)$ may be negative and can not be used as a probability distribution function.

[8]We use the same notation $M_\sigma(x)$ to denote the $N \times N$ matrix as defined in (1.4.26), and $NL \times NL$ matrix as defined in (1.4.31). It depends on the context which one we should use.

Then[9]

$$\det[M_\sigma(x)] = \det[I + B_{L,\sigma}(x_L)B_{L-1,\sigma}(x_{L-1})\cdots B_{1,\sigma}(x_1)]. \tag{1.4.33}$$

2. If A is a $N \times N$ symmetric and positive definite matrix, then[10].

$$\int e^{-v^T A^{-1} v} dv = (\sqrt{\pi})^N \det(A^{\frac{1}{2}}), \tag{1.4.34}$$

The identity can be proven by using the eigendecomposition of A.

Now, by introducing two auxiliary scalar fields Φ_σ for $\sigma = \pm$, we have

$$|\det[M_\sigma(x)]| = \det\left[M_\sigma^T(x)M_\sigma(x)\right]^{\frac{1}{2}} = \pi^{-\frac{NL}{2}} \int e^{-\Phi_\sigma^T O_\sigma^{-1}(x)\Phi_\sigma}, \tag{1.4.35}$$

where

$$O_\sigma(x) = M_\sigma(x)^T M_\sigma(x).$$

By combining (1.4.25) and (1.4.35), we see the expression (1.4.25) of the partition function Z_x can be recast as the following[11]

$$\begin{aligned} Z_x &= (C_2)^{NL} \int [\delta x] e^{-S_B(x)} \det[M_+(x)] \det[M_-(x)] \\ &= \left(\frac{C_2}{\pi}\right)^{NL} \int [\delta x \delta\Phi_+ \delta\Phi_-] e^{-\left(S_B(x) + \Phi_+^T O_+^{-1}(x)\Phi_+ + \Phi_-^T O_-^{-1}(x)\Phi_-\right)} \\ &\equiv \left(\frac{C_2}{\pi}\right)^{NL} \int [\delta x \delta\Phi_\sigma] e^{-V(x,\Phi_\sigma)}, \end{aligned}$$

where

$$V(x,\Phi_\sigma) = S_B(x) + \Phi_+^T O_+^{-1}(x)\Phi_+ + \Phi_-^T O_-^{-1}(x)\Phi_-. \tag{1.4.36}$$

Now let us consider how to move the configuration x which satisfies the distribution:

$$P(x,\Phi_\sigma) \propto \frac{1}{Z_x} e^{-V(x,\Phi_\sigma)}.$$

Similar to the DQMC method, for each Monte Carlo step, one can try to move $x = \{x_{\ell,i}\}$ at every spatial site i and imaginary time ℓ. An alternative efficient way is to move the entire configuration x by adding a Gaussian noise

$$x \longrightarrow x + \Delta x$$

[9]The identity can be easily derived based on the following observation: If a matrix A is a 2×2 block matrix,

$$A = \begin{bmatrix} A_{11} & A_{12} \\ A_{21} & A_{22} \end{bmatrix},$$

then $\det(A) = \det(A_{22})\det(F_{11}) = \det(A_{11})\det(F_{22})$, where $F_{11} = A_{11} - A_{12}A_{22}^{-1}A_{21}$ and $F_{22} = A_{22} - A_{21}A_{11}^{-1}A_{12}$

[10]The identity can be proven by using the eigen-decomposition of A. For example, see page 97 of [R. Bellman, Introduction to Matrix Analysis, SIAM Edition, 1997]

[11]Here we assume that $\det M_\sigma(x)$ is positive. Otherwise, we will have the so-called "sign problem".

where

$$\Delta x = -\frac{\partial V(x,\Phi_\sigma)}{\partial x}\Delta t + \sqrt{\Delta t}\, w_t,$$

Δt is one parameter with small value, and w_t follows a Gaussian distribution. This method is called Langevin-Euler moves, for example, see [9, p.192].

Spurred by the popularity of the molecular dynamics (MD) method, Scalettar *et al* [14] proposed a hybrid method to move x by combining Monte Carlo and molecular dynamics (MD), which is referred to as a Hybrid Quantum Monte Carlo (HMQC) simulation. In HQMC, an additional auxiliary momentum field $p = \{p_{\ell,i}\}$ is introduced. By the identity

$$\int_{-\infty}^{\infty} e^{z^2} dz = \sqrt{\pi},$$

we see that the partition function Z_x can be rewritten as

$$\begin{aligned} Z_x &= \left(\frac{C_2}{\pi}\right)^{NL} \int [\delta x \delta \Phi_\sigma] e^{-V(x,\Phi_\sigma)} \\ &= (C_2)^{NL} \pi^{-\frac{3NL}{2}} \int [\delta x \delta p \delta \Phi_\sigma] e^{-\left(\sum_{\ell,i} p_{\ell,i}^2 + V(x,\Phi_\sigma)\right)} \\ &\equiv (C_2)^{NL} \pi^{-\frac{3NL}{2}} \int [\delta x \delta p \delta \Phi_\sigma] e^{-H(x,p,\Phi_\sigma)} \equiv Z_H, \end{aligned}$$

where

$$H(x,p,\Phi_\sigma) = p^T p + V(x,\Phi_\sigma). \tag{1.4.37}$$

In summary, we seek the field configurations $\{x, p, \Phi_\sigma\}$ that obey the following probability distribution:

$$\{x,p,\Phi_\sigma\} \sim P(x,p,\Phi_\sigma) = \frac{1}{Z_H} e^{-H(x,p,\Phi_\sigma)}, \tag{1.4.38}$$

The hybrid Monte Carlo (HMC) combines the ideas of MD and the Metropolis acceptance-rejection rule to produce Monte Carlo samples from the target distribution (1.4.38).

1. Φ_σ is updated by simple MC:

   $$\Phi_\sigma = M_\sigma^T R_\sigma.$$

   where R_σ are two vectors of Gaussian random number, each component of which has a probability distribution proportional to $\exp(-R_{i,\sigma}^2)$.

2. (x, p) is updated by MD:

   Take the current x as an initial value $x(0)$, and set $p(0)$ whose entries $p_{\ell,i}$ are Gaussian random numbers with probability distribution proportional to $\exp(-p_{\ell,i}^2)$.

   Then we move to a new configuration $(x(T), p(T))$ satisfying the Hamiltonian equations

   $$\dot{p}_{\ell,i} = -\frac{\partial H}{\partial x_{\ell,i}} = -\frac{\partial V}{\partial x_{\ell,i}}, \tag{1.4.39}$$

   $$\dot{x}_{\ell,i} = \frac{\partial H}{\partial p_{\ell,i}} = 2p_{\ell,i} \tag{1.4.40}$$

Note that the fields Φ_σ and p are auxiliary fields. We first fix the fields Φ_σ, vary the fields p, and move (x, p) together. It is possible to use different moving order. We also note that from Liouville's theorem, see [1, Chap.3] or [11, Chap.2], we move along a trajectory in which both H and the differential volume element in phase space are constant and the system is equilibrium.

The leap-frog method, for example see [3], is a simple and efficient numerical method to move the configuration $(x(0), p(0))$ to $(x(T), p(T))$ satisfying the Hamiltonian equations (1.4.39) and (1.4.40).

For a small time step Δt, a molecular dynamics step keeps H constant. One can view this as a type of Monte Carlo move in which the energy does not change. The Metropolis algorithm tells us such a move should be accepted with probability one. Unfortunately, we have to use finite Δt and so H is not precisely constant. In order to keep the simulation from being biased by this fact, we need to use a Metropolis acceptance-rejection step.

The following is an outline of the Hybrid Quantum Monte Carlo (HQMC) method.

HQMC

1. Initialize
   - $x(0) = 0$,
   - $\Phi_\sigma = M_\sigma^T(x(0))R_\sigma$, where the entries $R_{\ell,i}$ of the vector R_σ are Gaussian random numbers with the probability distribution proportional to $\exp(-R_{i,\sigma}^2)$.
2. MC loop (total number of MC steps = warmup steps + measurement steps)
   (a) MD: $x(0) \longrightarrow x(T)$ by the leap-frog method, with stepsize Δt.
      i. Initialize p: $p(0) = (p_{\ell,i})$, where $p_{\ell,i}$ are Gaussian random numbers with probability distribution proportional to $\exp(-p_{i,l}^2)$. and then p is evolved through a half time step $\frac{1}{2}\Delta t$:

$$p_{\ell,i}(\frac{1}{2}\Delta t) = p_{\ell,i}(0) - \frac{\partial V(x(0), \Phi_\sigma)}{\partial x_{\ell,i}} \left(\frac{1}{2}\Delta t\right).$$

      ii. Perform MD steps:

$$x_{\ell,i}(t + \Delta t) - x_{i,l}(t) = 2p_{\ell,i}(t + \frac{1}{2}\Delta t)\Delta t,$$
$$p_{\ell,i}(t + \frac{3}{2}\Delta t) - p_{\ell,i}(t + \frac{1}{2}\Delta t) = -\frac{\partial V(x(t + \Delta t), \Phi_\sigma)}{\partial x_{\ell,i}}\Delta t.$$

   (b) Metropolis acceptance-rejection: generate a random number $r \sim \text{Uniform}[0, 1]$ and update

$$x(T) = \begin{cases} x(T), & \text{if } r \leq \min\left\{1, \frac{e^{-H(x(T),p(T),\Phi_\sigma)}}{e^{-H(x(0),p(0),\Phi_\sigma)}}\right\} \\ x(0), & \text{otherwise.} \end{cases}$$

   (c) Perform heat-bath step: $\Phi_\sigma = M_\sigma^T(x(T))R_\sigma$, where the entries $R_{\ell,i}$ of the vector R_σ are Gaussian random numbers with the probability distribution proportional to $\exp(-R_{i,\sigma}^2)$,
   (d) Perform physical measurements, after warmup steps
   (e) set $x(0) := x(T)$, goto MD step.

Remark **1.4.1** *The Langevin-Euler update is equivalent to a single-step HQMC move [9]. The MD and Langevin are two alternate methods which both have the virtue of moving all the variables together. Which is better depends basically on which allows the larger step size, the fastest evolution of the Hubbard-Stratonovich fields to new values.*

To this end, let us consider how to compute the force term $\frac{\partial V(x,\Phi_\sigma)}{\partial x_{\ell,i}}$. By the definition of $V(x,\Phi_\sigma)$ in (1.4.36), we first examine

$$\frac{\partial[\Phi_\sigma^T O_\sigma^{-1}(x)\Phi_\sigma]}{\partial x_{\ell,i}} = -\Phi_\sigma^T O_\sigma^{-1}(x)\frac{\partial O_\sigma(x)}{\partial x_{\ell,i}}O_\sigma^{-1}(x)\Phi_\sigma = -X_\sigma^T\frac{\partial O_\sigma(x)}{\partial x_{\ell,i}}X_\sigma,$$

where $X_\sigma = O_\sigma^{-1}(x)\Phi_\sigma$. Since $O_\sigma(x) = M_\sigma^T(x)M_\sigma(x)$, it follows that

$$X_\sigma^T\frac{\partial O_\sigma(x)}{\partial x_{\ell,i}}X_\sigma = 2(M_\sigma(x)X_\sigma)^T\frac{\partial M_\sigma(x)}{\partial x_{\ell,i}}X_\sigma.$$

By the expression (1.4.32) of the matrix $M_\sigma(x)$, we have

$$\frac{\partial M_\sigma(x)}{\partial x_{\ell,i}} = -K_{[L]}\frac{\partial V_{[L]}(x)}{\partial x_{\ell,i}}\Pi.$$

Note that $V_{[L]}(x)$ is a diagonal matrix, and only the (ℓ,i)-diagonal element $v_{\ell,i,\sigma} = \exp(-\sigma\tau(2U)^{\frac{1}{2}}x_{\ell,i})$ depends on $x_{\ell,i}$, therefore, we have

$$X_\sigma^T\frac{\partial O_\sigma(x)}{\partial x_{\ell,i}}X_\sigma = -2\frac{\partial v_{\ell,i,\sigma}}{\partial x_{\ell,i}}(K_{[L]}^T M_\sigma(x)X_\sigma)_{\ell,i}(\Pi X_\sigma)_{\ell,i}.$$

Therefore, we have

$$\begin{aligned}\frac{\partial V(x,\Phi_\sigma)}{\partial x_{\ell,i}} = 2\tau x_{\ell,i} \quad &- \quad 2(2U)^{\frac{1}{2}}\tau v_{\ell,i,+}(K_{[L]}^T M_+(x)O_+^{-1}(x)\Phi_+)_{\ell,i}(\Pi O_+^{-1}(x)\Phi_+)_{\ell+1,i} \\ &+ \quad 2(2U)^{\frac{1}{2}}\tau v_{\ell,i,-}(K_{[L]}^T M_-(x)O_-^{-1}(x)\Phi_-)_{\ell,i}(\Pi O_-^{-1}(x)\Phi_-)_{\ell+1,i}.\end{aligned}$$

1.4.3 Physical measurements

In section 1.3.3 we described how measurements are made in a determinant QMC code. The procedure in hybrid QMC is identical in that one expresses the desired quantities in terms of precisely the same products of Green's functions. The only difference is that these Green's functions are obtained from products of the vectors instead of directly from a matrix for G. The basic identity is this:

$$2\langle X_{\sigma,i}R_{\sigma,j}\rangle \leftrightarrow (M_\sigma)_{i,j}^{-1} = G_{ij}^\sigma. \tag{1.4.41}$$

This follows from the fact that

$$X_\sigma = O_\sigma^{-1}(x)\Phi_\sigma = M_\sigma^{-1}(x)R_\sigma$$

and that the components R_i of R_σ are independently distributed Gaussian random numbers $\langle R_i R_j\rangle = \frac{1}{2}\delta_{i,j}$.

Hence, the expression for the spin-spin correlation function would become

$$\langle c(l)\rangle = \langle c^{\dagger}_{i+l,\downarrow} c_{i+l,\uparrow} c^{\dagger}_{i,\uparrow} c_{i,\downarrow}\rangle = G^{\uparrow}_{i+l,i}\, G^{\downarrow}_{i,i+l} \leftrightarrow 4\,\langle R_{\uparrow,i+l} X_{\uparrow,i} R_{\downarrow,i} X_{\downarrow,i+l}\rangle. \tag{1.4.42}$$

The only point to be cautious of concerns the evaluation of expectation values of four fermion operators if the operators have the same spin index. There it is important that two different vectors of random numbers are used: R_σ, X_σ and R'_σ, X'_σ. Otherwise the averaging over the Gaussian random numbers generates additional, unwanted, values: $\langle R_i R_j R_k R_l\rangle = \frac{1}{4}(\delta_{i,j}\delta_{k,l} + \delta_{i,k}\delta_{j,l} + \delta_{i,l}\delta_{j,k})$, whereas $\langle R'_i R'_j R_k R_l\rangle = \frac{1}{4}\delta_{i,j}\delta_{k,l}$.

It should be apparent that if the indices i and j are in the same N dimensional block, we get the "'equal-time" Green's function

$$G_\sigma = M_\sigma^{-1} = [I + B_{L,\sigma} B_{L-1,\sigma} \cdots B_{1,\sigma}]^{-1}, \tag{1.4.43}$$

which is the quantity used in traditional determinant QMC.

However, choosing i, j in different N dimensional blocks, we can also access the non-equal time Green's function,

$$G_{\ell_1,i;\ell_2,j} = \langle c_i(\ell_1) c^{\dagger}_j(\ell_2)\rangle = (B_{\ell_1} B_{\ell_1-1} \cdots B_{\ell_2+1} (I + B_{\ell_2} \cdots B_1 B_L \cdots B_{\ell_2+1})^{-1})_{ij}.$$

At every measurement step in the HQMC simulation, the equal-time Green's function G_{ij} can be obtained from the diagonal block of M_σ^{-1} and the unequal-time Green's function $G_{\ell_1,i;\ell_2,j}$ can be computed from the (ℓ_1, ℓ_2) block submatrix of M_σ^{-1}.

As we already remarked in describing the measurements in determinant QMC, it is often useful to generalize the definition of correlation functions so that the pair of operators are separated in imaginary time as well as spatially. The values of the non-equal time Greens function allow us to evaluate these more general correlation functions $c(l, \tau)$. To motivate their importance we comment that just as the structure factor $S(q)$, the Fourier transform of the real space correlation function $c(l)$, describes the scattering of particles with change in momentum q, the Fourier transform of $c(l, \tau)$ into what is often called the susceptibility $\chi(q, \omega)$, tells us about scattering events where the momentum changes by q and the energy changes by ω.

1.5 Appendix A Updating Algorithm in DQMC

In this appendix, we discuss the single-state MC updating algorithm to provide a fast means to compute the Metropolis ratio in DQMC, as described in section 1.3.2.

A.1 Rank-one updates

Consider matrices M_1 and M_2 of the forms

$$M_1 = I + FV_1 \quad \text{and} \quad M_2 = I + FV_2,$$

where F is a given matrix. V_1 and V_2 are diagonal and nonsingular, and moreover, they differ only at the (1,1)-element, i.e.,

$$V_1^{-1}V_2 = I + \alpha_1 e_1 e_1^T, \quad \alpha_1 = \frac{V_2(1,1)}{V_1(1,1)} - 1,$$

where e_1 is the first column of the identity matrix I.

It is easy to see that M_2 is a rank-one update of M_1:

$$\begin{aligned} M_2 &= I + FV_1 + FV_1(V_1^{-1}V_2 - I) \\ &= M_1 + \alpha_1(M_1 - I)e_1 e_1^T \\ &= M_1\left[I + \alpha_1(I - M_1^{-1})e_1 e_1^T\right]. \end{aligned}$$

Therefore, the ratio of the determinants of the matrices M_1 and M_2 are given by[12]

$$r_1 = \frac{\det M_2}{\det M_1} = 1 + \alpha_1(1 - e_1^T M_1^{-1} e_1). \tag{1.5.44}$$

Therefore, computing the ratio r_1 is essentially about computing the (1,1)-element of the inverse of the matrix M_1.

By Sherman-Morrison formula, we see that the inverse of the matrix M_2 is a rank-one update of M_1^{-1}:

$$M_2^{-1} = \left[I - \frac{\alpha_1}{r_1}(I - M_1^{-1})e_1 e_1^T\right] M_1^{-1} = M_1^{-1} - \left(\frac{\alpha_1}{r_1}\right) u_1 v_1^T, \tag{1.5.45}$$

where the vectors u_1 and v_1 are defined by $u_1 = (I - M_1^{-1})e_1$ and $v_1 = M_1^{-T}e_1$.

Now, let us consider a sequence of matrices M_{i+1} generated by the rank-one update:

$$M_{i+1} = I + FV_{i+1}$$

where

$$V_i^{-1}V_{i+1} = I + \alpha_i e_i e_i^T, \quad \alpha_i = \frac{V_{i+1}(i,i)}{V_i(i,i)} - 1.$$

[12] Here we use the fact that $\det(I + xy^T) = 1 + y^T x$ for any two column vectors x and y.

for $i = 1, 2, \ldots, n-1$. Then by equation (1.5.44), we immediately have

$$r_i = \frac{\det M_{i+1}}{\det M_i} = 1 + \alpha_i(1 - e_i^T M_i^{-1} e_i),$$

and

$$M_{i+1}^{-1} = M_i^{-1} - \left(\frac{\alpha_i}{r_i}\right) u_i v_i^T,$$

where $u_i = (I - M_i^{-1})e_i$ and $v_i = M_i^{-T} e_i$.

Denote

$$U_k = [u_1, u_2, \cdots, u_{k-1}] \quad \text{and} \quad W = [w_1, w_2, \cdots, w_{k-1}].$$

then it is easy to see that the inverse of M_k can be written as a rank-$(k-1)$ update of M_1^{-1}:

$$M_k^{-1} = M_1^{-1} - U_{k-1} D_k W_{k-1}^T.$$

where $D_k = \text{diag}(\frac{\alpha_1}{r_1}, \frac{\alpha_2}{r_2}, \ldots, \frac{\alpha_{k-1}}{r_{k-1}})$.

Remark **1.5.1** *The discussion on the stability of such continuous updating can be found in [G.W.Stewart, Modifying pivot elements in Gaussian Elimination, Math. Comp., 28 (126)(1974), pp.537-542] and [E.L.Yip, A note on the stability of solving a rank-p modification of a linear system by the Sherman-Morrison-Woodbury formula, SIAM J.Sci.Stat.Comput., 7(2)(1986), pp.507-513].*

A.2 Computing the Metropolis ratio and updating the Green's function

As we discussed in section 1.3.2, in the DQMC, it is necessary to repeatedly compute the Metropolis ratio

$$r = \frac{\det[M_+(h')] \det[M_-(h')]}{\det[M_+(h)] \det[M_-(h)]},$$

for configurations h' and h, where $M_\sigma(h)$ is defined in (1.3.18), namely

$$M_\sigma(h) = I + B_{L,\sigma}(h_L) B_{L-1,\sigma}(h_{L-1}) \cdots B_{2,\sigma}(h_2) B_{1,\sigma}(h_1).$$

Note that $h = (h_1, h_2, \ldots, h_L)$, $h' = (h'_1, h'_2, \ldots, h'_L)$, and each h_ℓ or h'_ℓ is a N-length vector.

The Green's function associated with the configuration h is defined as

$$G_\sigma(h) = M_\sigma^{-1}(h)$$

DQMC update of configuration h. We consider the DQMC simulation where the elements of configurations h' and h are the same except at the imaginary time slice ℓ and spatial site i:

$$h'_{\ell,i} = -h_{\ell,i},$$

i.e., configuration h' is obtained by a simple flip at (ℓ, i). This update is done for $\ell = 1, 2, \ldots, L$ and $i = 1, 2, \ldots, N$.

Let us start with the imginary time slice $\ell = 1$:

- at the spatial site $i = 1$:

$$h'_{1,1} = -h_{1,1}.$$

By the relationship between $M_\sigma(h')$ and $M_\sigma(h)$ and equation (1.5.44), one can derive that the Metropolis ratio r_{11} is given by

$$r_{11} = d_+ d_-, \tag{1.5.46}$$

where for $\sigma = \pm$,

$$d_\sigma = 1 + \alpha_{1,\sigma}\left(1 - e_1^T M_\sigma^{-1}(h) e_1\right) = 1 + \alpha_{1,\sigma}\left(1 - (G_\sigma(h))_{11}\right),$$

and

$$\alpha_{1,\sigma} = e^{-2\sigma\nu h_{1,1}} - 1.$$

Therefore, the gist of computing the Metropolis ratio r_{11} is to compute the $(1,1)$-element of the inverse of the matrix $M_\sigma(h)$.

If the Green's function $G_\sigma(h)$ has been computed explicitly in advance, then it is essentially "free" to compute the ratio r_{11}. In this case, if the proposed h' is accepted, then by the equality (1.5.45), the Green's function $G_\sigma(h)$ is updated by a rank-one matrix:

$$G_\sigma(h) \leftarrow G_\sigma(h) - \frac{\alpha_{1,\sigma}}{r_{11}}\, u_\sigma w_\sigma^T.$$

where

$$u_\sigma = (I - G_\sigma(h))e_1 \quad \text{and} \quad w_\sigma = G_\sigma^T(h)e_1.$$

- At the site $i = 2$:

$$h'_{1,2} = -h_{1,2}.$$

By the similar derivation as for the previous case $(\ell, i) = (1,1)$, we have

$$r_{12} = d_+ d_-, \tag{1.5.47}$$

where for $\sigma = \pm$,

$$d_\sigma = 1 + \alpha_{2,\sigma}\left(1 - (G_\sigma(h))_{12}\right), \quad \alpha_{1,\sigma} = e^{-2\sigma h_{1,2}} - 1.$$

Correspondingly, if necessary, the Green's function is updated by the rank-one matrix

$$G_\sigma(h) \leftarrow G_\sigma(h) - \frac{\alpha_i}{r_{12}}\, u_\sigma w_\sigma^T.$$

where

$$u_\sigma = (I - G_\sigma(h))e_1 \quad \text{and} \quad w_\sigma = G_\sigma^T(h)e_1.$$

- It is immediately seen that for the time slice $\ell = 1$, we can use same procedure for computing the Metropolis ratios r_{1i} for $i = 3, 4, \ldots, N$, and updating the Green's function $G_\sigma(h)$.

- For high performance computing, one may delay the update of the Green's functions t to lead to a block high rank update, instead of rank-one update. There is a so-called "delayed update" technique.

Now, let us consider how to do the DQMC configuration update for the time slice $\ell = 2$. We first notice that the matrices $M_\sigma(h)$ and $M_\sigma(h')$ can be rewritten as

$$\begin{aligned} M_\sigma(h) &= B_{1,\sigma}^{-1}(h_1)\widehat{M}_\sigma(h)B_{1,\sigma}(h_1) \\ M_\sigma(h') &= B_{1,\sigma}^{-1}(h_1')\widehat{M}_\sigma(h')B_{1,\sigma}(h_1') \end{aligned}$$

where

$$\begin{aligned} \widehat{M}_\sigma(h) &= I + B_{1,\sigma}(h_1)B_{L,\sigma}(h_L)B_{L-1,\sigma}(h_{L-1})\cdots B_{2,\sigma}(h_2) \\ \widehat{M}_\sigma(h') &= I + B_{1,\sigma}(h_1')B_{L,\sigma}(h_L')B_{L-1,\sigma}(h_{L-1}')\cdots B_{2,\sigma}(h_2'). \end{aligned}$$

Consequently, the Metropolis ratio r can be written as

$$r_{2i} = \frac{\det[M_+(h')]\det[M_-(h')]}{\det[M_+(h)]\det[M_-(h)]} = \frac{\det[\widehat{M}_+(h')]\det[\widehat{M}_-(h')]}{\det[\widehat{M}_+(h)]\det[\widehat{M}_-(h)]}.$$

and the associated Green's function is updated via a "wrapping":

$$\widehat{G}_\sigma(h) \leftarrow B_{1,\sigma}^{-1}(h_1)G_\sigma(h)B_{1,\sigma}(h_1).$$

We see now that the configurations h_2 and h_2' associated with the time slice $\ell = 2$ appear at the same location as the the configurations h_1 and h_1' at the time slice $\ell = 1$. Therefore, we can use the same formulation as for the time slice $\ell = 1$ to compute the Metropolis ratios r_{2i} and update the associated Greent's functions.

When $\ell \geq 3$, it is clear that we can repeat the previous discussion for computing the Metropolis ratios $r_{\ell i}$ iand updating the associated Green's function for the time slices $\ell = 3, 4, \ldots, L$, and the spatial sites $i = 1, 2, \ldots, N$.

Remark **1.5.2** *As we noticed that the main computing costs is on the updating of Green's functions. It costs $2N^2$ flops at each spatial site i. The total cost of one-loop (for the flippings of all NL sites) is $\mathcal{O}(2N^3L)$.*

One important problem is how to numerically stable and efficient to compute the initial Green's function $G_\sigma(h)$, and to recompute the Green's functions after a certain number of updating steps for numerical accuracy. The QR decomposition with pivoting is currently used in the DQMC implementation [10].

1.6 Appendix B Particle-Hole Transformation

In this appendix, we give an algebraic derivation for the so-called *particle-hole transformation*.

B.1 Algebraic identities

we first present a few algebraic identities.

Lemma 1.6.1 *For any nonsingular matrix A,*

$$(I + A^{-1})^{-1} = I - (I + A)^{-1}.$$

Lemma 1.6.2 *Let the matrices A_ℓ be symmetric and nonsingular for $\ell = 1, 2, \cdots, m$, then*

$$(I + A_m^{-1} A_{m-1}^{-1} \cdots A_1^{-1})^{-1} = I - (I + A_m A_{m-1} \cdots A_1)^{-T}.$$

Theorem 1.6.1 *For any square matrices A and B, if there exists a nonsingular matrix Π such that*

$$\Pi A + A\Pi = 0 \quad \textit{and} \quad \Pi B - B\Pi = 0,$$

namely, Π anti-commutes with A and commutes with B. Then we have

$$(I + e^{A-B})^{-1} = I - \Pi^{-1}(I + e^{A+B})^{-1}\Pi \tag{1.6.48}$$

and

$$\det(I + e^{A-B}) = e^{\mathrm{Tr}(A-B)} \det(I + e^{A+B}) \tag{1.6.49}$$

Proof. First, we prove the inverse identity (1.6.48),

$$\begin{aligned} (I + e^{A-B})^{-1} &= I - (I + e^{-A+B})^{-1} = I - (I + e^{\Pi^{-1}(A+B)\Pi})^{-1} \\ &= I - (I + \Pi^{-1} e^{A+B} \Pi)^{-1} = I - \Pi^{-1}(I + e^{A+B})^{-1}\Pi. \end{aligned}$$

Now, let us prove the determinant identity (1.6.49). Note that

$$\begin{aligned} I + e^{A-B} &= e^{A-B}(I + e^{-(A-B)}) = e^{A-B}(I + e^{-A+B}) \\ &= e^{A-B}(I + e^{\Pi^{-1}A\Pi + \Pi^{-1}B\Pi}) = e^{A-B}(I + \Pi^{-1} e^{A+B}\Pi) \\ &= e^{A-B}\Pi^{-1}(I + e^{A+B})\Pi. \end{aligned}$$

Hence, we have

$$\begin{aligned} \det(I + e^{A-B}) &= \det e^{A-B} \cdot \det \Pi^{-1} \cdot \det(I + e^{A+B}) \cdot \det \Pi \\ &= e^{\mathrm{Tr}(A-B)} \det(I + e^{A+B}). \end{aligned}$$

For the last equality, we used the identity $\det e^W = e^{\mathrm{Tr}W}$ for any square matrix W. ∎

The following theorem gives the relations of the inverses and determinants of the matrices $I + e^A e^{-B}$ and $I + e^A e^B$.

Theorem 1.6.2 *For symmetric matrices A and B, if there exists a nonsingular matrix Π such that*

$$\Pi A + A\Pi = 0 \quad \textit{and} \quad \Pi B - B\Pi = 0.$$

Then we have

$$(I + e^A e^{-B})^{-1} = I - \Pi^{-T}(I + e^A e^B)^{-T}\Pi^T \tag{1.6.50}$$

and

$$\det(I + e^A e^{-B}) = e^{\mathrm{Tr}(A-B)} \det(I + e^A e^B) \tag{1.6.51}$$

The following theorem is a generalization of Theorem 1.6.2.

Theorem 1.6.3 *Let $M_\sigma = I + e^A e^{\sigma B_k} e^A e^{\sigma B_{k-1}} \cdots e^A e^{\sigma B_1}$, where A and $\{B_\ell\}$ are symmetric, $\sigma = +, -$. If there exists a nonsingular matrix Π that anti-commutes with A and commutes with B_ℓ, i.e.,*

$$\Pi A + A\Pi = 0 \quad \textit{and} \quad \Pi B_\ell - B_\ell \Pi = 0 \quad \textit{for } \ell = 1, 2, \ldots, k.$$

Then we have

$$M_-^{-1} = I - \Pi^{-T} M_+^{-T} \Pi^T \tag{1.6.52}$$

and

$$\det(M_-) = e^{k\mathrm{Tr}(A) - \sum_{\ell=1}^k \mathrm{Tr}(B_\ell)} \det(M_+) \tag{1.6.53}$$

The following theorem is another generalization of Theorem 1.6.2.

Theorem 1.6.4 *Let A and B be symmetric matrices, and W be a nonsingular matrix. If there exists a nonsingular matrix Π such that it anti-commutes with A and commutes with B, i.e.,*

$$\Pi A + A\Pi = 0 \quad \textit{and} \quad \Pi B - B\Pi = 0$$

and furthermore, it satisfies the identity

$$\Pi = W\Pi W^T.$$

Then

$$(I + e^A e^{-B} W)^{-1} = I - \Pi^{-T}(I + e^A e^B W)^{-T}\Pi^T \tag{1.6.54}$$

and

$$\det(I + e^A e^{-B} W) = e^{\mathrm{Tr}(A-B)} \cdot \det W \cdot \det(I + e^A e^B W) \tag{1.6.55}$$

B.2 Particle-hole transformation in DQMC

1-D lattice. Consider the simple 1-D lattice with N_x site, with

$$K_x = \begin{bmatrix} 0 & 1 & & & 1 \\ 1 & 0 & 1 & & \\ & 1 & 0 & 1 & \\ & & \ddots & \ddots & \ddots \\ 1 & & & 1 & 0 \end{bmatrix}_{N_x \times N_x}.$$

and $N_x \times N_x$ diagonal matrices V_ℓ for $\ell = 1, 2, \ldots, L$.

If N_x is even, then the matrix

$$\Pi_x = \mathrm{diag}(1, -1, 1, -1, \ldots, 1, -1)$$

is anti-commutible with K_x and is commutible with V_ℓ, i.e.,

$$\Pi_x K_x + K_x \Pi_x = 0 \quad \text{and} \quad \Pi_x V_\ell - V_\ell \Pi_x = 0 \quad \text{for} \quad \ell = 1, 2, \ldots, L.$$

Then by Theorem 1.6.3, the determinants of the matrices M_- and M_+ satisfy the relation

$$\det(M_-) = e^{-\sum_{\ell=1}^{L} \mathrm{Tr}(V_\ell)} \det(M_+).$$

For the Green's functions:

$$G_\sigma = M_\sigma^{-1} = (I + e^{\tau t K_x} e^{\sigma V_L} e^{\tau t K_x} e^{\sigma V_{L-1}} \cdots e^{\tau t K_x} e^{\sigma V_1})^{-1}$$

where $\sigma = +$ or $-$, we have

$$G_- = I - \Pi_x G_+^T \Pi_x.$$

This is referred to as the *particle-hole transformation* in the condensed matter physics literature.

2-D rectangle lattice. Consider a 2-D rectangle lattice with $N_x \times N_y$ sites, where

$$K = K_x \otimes I + I \otimes K_y.$$

and $N_x N_y \times N_x N_y$ diagonal matrices V_ℓ for $\ell = 1, 2, \ldots, L$.

If N_x and N_y are even, then the matrix

$$\Pi = \Pi_x \otimes \Pi_y$$

is anti-communtible with K and is communtible with V_ℓ:

$$\Pi K + K \Pi = 0 \quad \text{and} \quad \Pi V_\ell - V_\ell \Pi = 0 \quad \text{for} \quad \ell = 1, 2, \ldots, L.$$

Then by Theorem 1.6.3, we have

$$\det(M_-) = e^{-\sum_{\ell=1}^{L} \mathrm{Tr}(V_\ell)} \det(M_+).$$

This is the identity we used in equation (1.4.28). Furthermore, for the Green's functions:

$$G_\sigma = M_\sigma^{-1} = (I + e^{\tau t K} e^{\sigma V_L} e^{\tau t K} e^{\sigma V_{L-1}} \cdots e^{\tau t K} e^{\sigma V_1})^{-1}$$

where $\sigma = +$ (spin up) or $-$ (spin down), we have

$$G_- = I - \Pi G_+^T \Pi.$$

This is referred to as the *particle-hole transformation* in the condensed matter physics literature.

B.3 Particle-hole transformation in HQMC

In the HQMC, we consider the matrix M_σ of the form

$$M_\sigma = \begin{bmatrix} I & & & & & e^{\tau t} K e^{\sigma V_1} \\ -e^{\tau t K} e^{\sigma V_2} & I & & & & \\ & -e^{\tau t K} e^{\sigma V_2} & I & & & \\ & & \ddots & \ddots & & \\ & & & -e^{\tau t} K e^{\sigma V_L} & & I \end{bmatrix} = I + e^A e^{\sigma D} P$$

where $A = \mathrm{diag}(\tau t K, \tau t K, \ldots, \tau t K)$ and $D = \mathrm{diag}(V_1, V_2, \ldots, V_L)$ and

$$P = \begin{bmatrix} 0 & & & & I \\ -I & 0 & & & \\ & -I & 0 & & \\ & & \ddots & \ddots & \\ & & & -I & 0 \end{bmatrix}.$$

It can be verify that for the 1-D or 2-D rectangle lattices, i.e., $K = K_x$ or $K = K_x \otimes I + I \otimes K_y$ as defined in B.2, the matrix

$$\Pi = I \otimes \Pi_x \quad \text{(1-D)}$$

or

$$\Pi = I \times \Pi_x \otimes P_y \quad \text{(2-D)}$$

anti-commutes with A and commutes with D, i.e.,

$$\Pi A + A \Pi = 0, \quad \Pi D - D \Pi = 0,$$

and furthermore, it satisfies

$$\Pi = P \Pi P^T.$$

Then by Theorem 1.6.4, the determinants of M_+ and M_- are related by

$$\det(M_-) = e^{-\sum_{\ell=1}^{L} \mathrm{Tr}(V_\ell)} \cdot \det(M_+).$$

Note that $\det P = 1$.

The Green's functions $G_+ = M_+^{-1}$ and $G_- = M_-^{-1}$ satisfy the relation

$$G_- = I - \Pi G_+^T \Pi.$$

Note that $\det P = 1$.

B.4 An open problem

Beside the 1-D and 2-D rectangle lattices, namely the lattice structure matrices K_x and K as defined in B.2, are there other types of lattices (and associated structure matrices K) such that we can apply Theorems 1.6.4 to establish the relationships between the inverses and determinants in the DQMC? It is known that for the honeycomb lattices, it is true, but for the triangle lattices, it is false.

A similar question is also valid for the HQMC.

B.5 Some useful basic identities

1. In general, $e^{A+B} \neq e^A e^B$, and $e^A e^B \neq e^B e^A$.
2. $(e^A)^{-1} = e^{-A}$ for every nonsingular matrix A
3. $e^{P^{-1}AP} = P^{-1} e^A P$
4. $(e^A)^H = e^{A^H}$ for every square matrix A

   e^A is Hermitian of A is Hermitian

   e^A is unitary of A is skew-Hermitian
5. $\det e^A = e^{\mathrm{Tr}A}$ for every square matrix A
6. $e^{A\otimes I + I\otimes B} = e^A \otimes e^B$

Bibliography

[1] V.I.Arnold, Mathematical Methods of Classical Mechanics, Graduate Texts in Mathematics 60, Second edition, Springer-Verlag, New York, 1989.

[2] R. Blankenbecler, D. J. Scalapino and R. L. Sugar, Phys. Rev. D, 24(1981), 2278-2286.

[3] Ernst Hairer, Christian Lubich and Gerhard Wanner, Geometric numerical integration illustrated by the Störmer-Verlet method, Acta Numerica (2003) 399-450.

[4] J. E. Hirsch, Two-dimensional Hubbard model: Numerical simulation study, Physical Review B, 31(7)(1985), 4403-4419.

[5] J. E. Hirsch, Hubbard-stratonovich transformation for fermion lattice models, PRB, 28(7)(1983),4059-4061.

[6] J. E. Hirsch, Erratum: Discrete Hubbard-Stratonovich transformation for fermion lattice models, PRB, 29(7)(1984), 4159.

[7] J. Hubbard, Electron Correlations in Narrow Energy Bands, Proc. R.Soc. London, Ser. A, 276(1963),238-257.

[8] J. Hubbard, Electron Correlations in Narrow Energy Bands III: An Improved solution, Proc. R.Soc. London, Ser. A, 281(1964), 401-419.

[9] Jun S. Liu, Monte Carlo Strategies in scientific computing, Spring series in statistics, 2001.

[10] E. Y. Loh Jr and J. E. Gubernatis, Stable numerical simulations of models of interacting electrons in Electronic Phase Transition edited by W. Hanks and Yu. V. Kopaev, Elsevier Science Publishers B. V., 1992, pp.177–235.

[11] R.K.Pathria, Statistical Mechanics, Second edition, Elsevier(Singapore),2001

[12] R. Schumann and E. Heiner, Transformations of the Hubbard interaction to quadratic forms, Physics Letters A, 134(3)(1988),202-204.

[13] D. J. Scalapino and R. L. Sugar, Phys. Rev. B, 24(1981),4295-4308.

[14] R. T. Scalettar, D. J. Scalapino, R. L. Sugar, and D. Toussaint, Hybrid molecular-dynamics algorithm for the numerical simulation of many-electron systems, Physical Review B, 36(1987),8632-8640.

[15] R. T. Scalettar, D. J. Scalapino and R. L. Sugar, New algorithm for the numerical simulation of fermions, Physical Review B, 34(1986),7911-7917.

[16] J. P. Wallington and J. F. Annett, Discrete symmetries and transformations of the Hubbard model, PRB, 58(3),1998,1218-1221.

Lecture 2

Hubbard matrix analysis

For developing robust and efficient algorithmic techniques and high performance software for the QMC simulations described in the previous lecture, it is important to understand mathematical and numerical properties of the underlying matrices, referred to as the Hubbard matrices, such as eigenvalue distribution and condition number. In this lecture, we study the dynamics and transitional behaviors of the properties of Hubbard matrices as functions of multiscale parameters.

2.1 Hubbard matrices

To simplify the notation, we write the matrix M introduced in the HQMC simulation of Lecture 1 as

$$M = \begin{bmatrix} I & & & & B_1 \\ -B_2 & I & & & \\ & -B_3 & I & & \\ & & \ddots & \ddots & \\ & & & -B_L & I \end{bmatrix}, \tag{2.1.1}$$

and refer to it as "Hubbard matrix", where

- I is a $N \times N$ unit matrix,
- B_ℓ is an $N \times N$ matrix of the form

$$B_\ell = e^{t\tau K} e^{V_\ell}. \tag{2.1.2}$$

- scalar t is a hopping parameter and $\tau = \frac{\beta}{L}$,
- K is a matrix describing lattice structure,
- V_ℓ is an $N \times N$ diagonal matrix, $V_\ell = \nu \cdot \mathrm{diag}(h_{\ell,1}, h_{\ell,2}, \ldots, h_{\ell,N})$, and ν is a parameters defined by $\cosh \nu = e^{\frac{U\tau}{2}}$. Note that $\nu = (\tau U)^{\frac{1}{2}} + \frac{1}{12}(\tau U)^{\frac{3}{2}} + \mathcal{O}((\tau U)^2)$.
- $\{h_{\ell,j}\}$ are random variables, referred to as Hubbard-Stratonovich field or configurations.

The Hubbard matrix M can be compactly written as

$$M = I_{NL} - \mathrm{diag}(B_1, B_2, \ldots, B_L)\Pi \tag{2.1.3}$$

or

$$M = I_{NL} - (I_N \otimes B)D_{[L]}(P \otimes I_N), \tag{2.1.4}$$

where I_N and I_{NL} are $N \times N$ and $NL \times NL$ unit matrices, respectively,

$$P = \begin{bmatrix} 0 & & & -1 \\ 1 & 0 & & \\ & \ddots & \ddots & \\ & & 1 & 0 \end{bmatrix}, \quad \Pi = P \otimes I_N = \begin{bmatrix} 0 & & & -I_N \\ I_N & 0 & & \\ & \ddots & \ddots & \\ & & I_N & 0 \end{bmatrix}.$$

and

$$\begin{aligned} B &= e^{t\tau K}, \\ D_{[L]} &= \mathrm{diag}(e^{V_1}, e^{V_2}, \ldots, e^{V_L}). \end{aligned}$$

The Hubbard matrix M displays *multi-length scale* properties, since the dimensions and properties of M are characterized by multiple length and energy parameters, and random variables. Specifically, we have

- Length parameters: N and L
  - N is the spatial size. If the density ρ is given, N also measures the number of electrons being simulated.
  - L is the number of blocks, it is set by the inverse of the temperature.
- Energy-scale parameters: t, U and β
  - t determines the hopping of electrons between different atoms in the solid and thus measures the material's kinetic energy.
  - U measures the strength of the interactions between the electrons, that is the potential energy.
  - β is the inverse-temperature.
- The parameter connecting length and energy scales: $\tau = \beta/L$.
  - τ is a discretization parameter, a measure of the accuracy of the Suzuki-Trotter decomposition.
- Configuration random variables $h_{\ell,j}$.

In more complex situations other energy scales also enter, such as the frequency of ionic vibrations (phonons) and the strength of the coupling of electrons to those vibrations.

In summary, the matrix M has the following features.

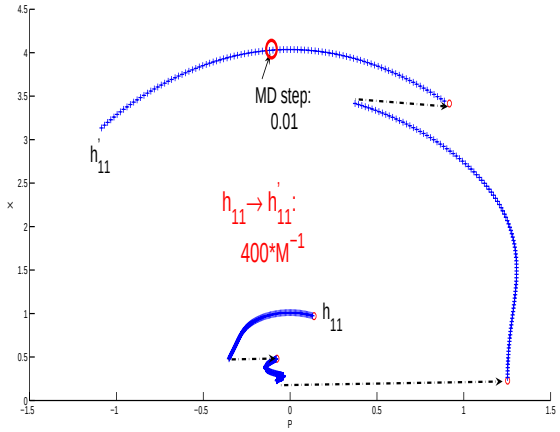

Figure 2.1: A typical MD trajectory in a HQMC simulation.

- M incorporates multiple structural scales: The inverse temperature β determines the number of blocks $L = \beta/\tau$, where τ is a discretization stepsize. Typically $L = 10$ to 10^2. The dimension of the individual blocks is set by N the number of spatial sites. In a typical 2D simulations $N = N_x \times N_y \propto 10^2 \sim 10^3$. Thus the dimension of the M is $10^4 \sim 10^5$.

- M incorporates multiple energy scales: The parameter t determines the kinetic energy of the electrons, and the interaction energy scale U determines the potential energy.

- M is a function of NL random variables $h_{\ell i}$, the so-called Hubbard-Stratonovich field. The goal of the simulation is to determine the configurations of these variables which make large contributions to operator expectation values, and then to sum over those configurations. Therefore, the associated matrix computation problems, such as computing $M^{-1}b$, need to be solved 10^4 to 10^5 times in a full simulation, see Figure 2.1, where at every step, we have the matrix computation problems.

The matrix computation problems which enter quantum simulations are the following:

1. Computation of the ratio of the determinants of the form $\frac{\det(\widehat{M})}{\det(M)}$, where $\widehat{M}$ is a low-rank update of M, see the Metropolis accept/reject decision in the DQMC algorithm and Appendix A of Lecture 1.

2. Solution of linear systems of the form $M^T M x = b$, see HQMC algorithm for molecular dynamics steps in Lecture 1.

3. Computation of specific elements of the inverse $(M^{-1})_{ij}$, for computing physical observables, such as energy, density, magnetic and moments, see sections 1.3.3 and 1.4.3.

One of computational challenges is to increase the spatial dimension $N = N_x \times N_y$ from $O(10^2)$ to $O(10^3)$, that is, to do a 1000 electron QMC simulation. Such an increase would

have a tremendous impact on our understanding of strongly interacting materials because it would allow for the first time the simulation of systems incorporating a reasonable number of the mesoscopic structures, such as a "checkerboard" electronic crystal[1] and stripes stripe structure arising from removing electrons from the filling of one electron per site in the Hubbard model[2]

2.2 Basic Properties

In this section, we exploit basic properties of the Hubbar matrix M as defined in (2.1.1).

1. A block LU factorization of M is given by

$$M = LU, \tag{2.2.5}$$

where

$$L = \begin{bmatrix} I & & & & \\ -B_2 & I & & & \\ & -B_3 & I & & \\ & & \ddots & \ddots & \\ & & & -B_L & I \end{bmatrix}$$

and

$$U = \begin{bmatrix} I & & & B_1 \\ & I & & B_2B_1 \\ & & \ddots & \vdots \\ & & I & B_{L-1}\cdots B_1 \\ & & & I + B_LB_{L-1}\cdots B_1 \end{bmatrix}$$

2. Note that the inverses of the factors L and U are given by

$$L^{-1} = \begin{bmatrix} I & & & & \\ B_2 & I & & & \\ B_3B_2 & B_3 & I & & \\ \vdots & \ddots & \ddots & \ddots & \\ B_LB_{L-1}\cdots B_2 & \cdots & B_LB_{L-1} & B_L & I \end{bmatrix}$$

and

$$U^{-1} = \begin{bmatrix} I & & & -B_1F \\ & I & & -B_2B_1F \\ & & \ddots & \vdots \\ & & I & -B_{L-1}\cdots B_1F \\ & & & F \end{bmatrix}$$

where $F = (I + B_LB_{L-1}\cdots B_2B_1)^{-1}$. Therefore, the inverse of M is explicitly given by

$$M^{-1} = U^{-1}L^{-1} = W^{-1}Z, \tag{2.2.6}$$

[1] T. Hanaguri *et al.* Nature 430, 1001 (2004)
[2] S.R. White *et al.*, Phys. Rev. Lett. 80, 1272(1998).

where

$$W = \mathrm{diag}(I + B_1 B_L \cdots B_2,\ I + B_2 B_1 B_L \cdots B_3,\ \ldots,\ I + B_L B_{L-1} \cdots B_1)$$

and

$$Z = \begin{bmatrix} I & -B_1 B_L \cdots B_3 & -B_1 B_L \cdots B_4 & \cdots & -B_1 B_L & -B_1 \\ B_2 & I & -B_2 B_1 B_L \cdots B_4 & \cdots & -B_2 B_1 B_L & -B_2 B_1 \\ B_3 B_2 & B_3 & I & \cdots & -B_3 B_2 B_1 B_L & -B_3 B_2 B_1 \\ \vdots & \vdots & \vdots & \vdots & \vdots & \vdots \\ B_{L-1} \cdots B_2 & B_{L-1} \cdots B_3 & B_{L-1} \cdots B_4 & \cdots & I & -B_{L-1} \cdots B_2 B_1 \\ B_L \cdots B_2 & B_L \cdots B_3 & B_L \cdots B_4 & \cdots & B_L & I \end{bmatrix},$$

In other words, the (i, j) block submatrix, denoted as $\{M\}_{ij}^{-1}$, of M^{-1} is given by

$$\{M^{-1}\}_{i,j} = (I + B_i \cdots B_1 B_L \cdots B_{i+1})^{-1} Z_{ij}$$

where

$$Z_{ij} = \begin{cases} B_i B_{i-1} \cdots B_{j+1}, & i > j \\ I, & i = j \\ -B_i \cdots B_1 B_L \cdots B_{j+1}, & i < j \end{cases}.$$

3. By the LU factorization (2.2.5), the following determinant identity holds:

$$\det(M) = \det(I + B_L B_{L-1} \cdots B_1). \tag{2.2.7}$$

2.3 Matrix exponential $B = e^{t\tau K}$

In this section, we discuss how to compute the matrix exponential $B = e^{t\tau K}$ when K defines a standard 2-D $N_x \times N_y$ rectangle lattice, i.e., .

$$K = I_y \otimes K_x + K_y \otimes I_x,$$

where I_x and I_y are unit matrices of dimensions N_x and N_y, respectively, and K_x and K_y are $N_x \times N_x$ and $N_y \times N_y$ matrices of the form

$$K_x, K_y = \begin{bmatrix} 0 & 1 & & & 1 \\ 1 & 0 & 1 & & \\ & \ddots & \ddots & \ddots & \\ & & 1 & 0 & 1 \\ 1 & & & 1 & 0 \end{bmatrix}.$$

First, by a straightforward calculation, we can verify the following lemma.

Lemma 2.3.1 *The eigenvalues of K are*

$$\kappa_{ij} = 2(\cos\theta_i + \cos\theta_j), \tag{2.3.8}$$

where

$$\begin{aligned}\theta_i &= \frac{2i\pi}{N_x}, \quad \textit{for} \quad i = 0, 1, 2, \ldots, N_x - 1 \\ \theta_j &= \frac{2j\pi}{N_y}, \quad \textit{for} \quad j = 0, 1, 2, \ldots, N_y - 1.\end{aligned}$$

The corresponding eigenvectors are

$$v_{ij} = u_j \otimes u_i,$$

where

$$\begin{aligned}u_i &= \frac{1}{\sqrt{N_x}}[1, e^{\mathrm{i}\theta_i}, e^{\mathrm{i}2\theta_i}, \ldots, e^{\mathrm{i}(N_x-1)\theta_i}]^T, \\ u_j &= \frac{1}{\sqrt{N_y}}[1, e^{\mathrm{i}\theta_j}, e^{\mathrm{i}2\theta_j}, \ldots, e^{\mathrm{i}(N_y-1)\theta_j}]^T.\end{aligned}$$

We now turn to the computation of the matrix exponential $B = e^{t\tau K}$.[3] By the definition of K, the matrix exponential $e^{t\tau K}$ can be written as the product of two matrix exponentials:

$$B = e^{t\tau K} = (I_y \otimes e^{t\tau K_x})(e^{t\tau K_y} \otimes I_x) = e^{t\tau K_y} \otimes e^{t\tau K_x}. \tag{2.3.9}$$

By Lemma 2.3.1, we can use the FFT to compute B. The computational complexity of formulating the matrix B explicitly is $O(N^2)$. The complexity of matrix-vector multiplication is $O(N(\log N_x + \log N_y))$.

Checkerboard approximation. In practice, we use an approximation of the matrix exponential $B = e^{t\tau K}$, when τ is sufficiently small. The method is referred to as *checkerboard approximation*[4]. It only costs $O(N)$. For simplicity, assume that N_x and N_y are even. Write K_x as

$$K_x = K_x^{(1)} + K_x^{(2)},$$

where

$$K_x^{(1)} = \begin{bmatrix} D & & & \\ & D & & \\ & & \ddots & \\ & & & D \end{bmatrix}, \quad K_x^{(2)} = \begin{bmatrix} 0 & & & 1 \\ & D & & \\ & & \ddots & \\ & & D & \\ 1 & & & 0 \end{bmatrix}, \quad D = \begin{bmatrix} 0 & 1 \\ 1 & 0 \end{bmatrix}.$$

Note that for any scalar $\alpha \neq 0$, the matrix exponential $e^{\alpha D}$ is given by

$$e^{\alpha D} = \begin{bmatrix} \cosh\alpha & \sinh\alpha \\ \sinh\alpha & \cosh\alpha \end{bmatrix}.$$

[3] A survey of the numerical methods to compute the matrix exponential is [Clever Moler and Charles Van Loan, Nineteen Dubious ways to compute the exponential of a matrix, twenty-five years later, SIAM Review, 45(2003),3-49.]

[4] It is particularly useful for different hopping t_{ij} at different lattices, i.e., t is not a constant.

Therefore, we have

$$e^{\alpha K_x^{(1)}} = \begin{bmatrix} e^{\alpha D} & & & \\ & e^{\alpha D} & & \\ & & \ddots & \\ & & & e^{\alpha D} \end{bmatrix}, \quad e^{\alpha K_x^{(2)}} = \begin{bmatrix} \cosh\alpha & & & \sinh\alpha \\ & e^{\alpha D} & & \\ & & \ddots & \\ & & e^{\alpha D} & \\ \sinh\alpha & & & \cosh\alpha \end{bmatrix}.$$

Since $K_x^{(1)}$ does not commute with $K_x^{(2)}$, we use the approximation

$$e^{\alpha K_x} = e^{\alpha K_x^{(1)}} e^{\alpha K_x^{(2)}} + O(\alpha^2),$$

where α is a scalar. Similarly, we have the approximation

$$e^{\alpha K_y} = e^{\alpha K_y^{(1)}} e^{\alpha K_y^{(2)}} + O(\alpha^2),$$

Subsequently, the matrix B has the approximation

$$\begin{aligned} B &= e^{t\tau K_y} \otimes e^{t\tau K_x} \\ &= (e^{t\tau K_y^{(1)}} e^{t\tau K_y^{(2)}}) \otimes (e^{t\tau K_x^{(1)}} e^{t\tau K_x^{(2)}}) + O(t^2\tau^2) \\ &\approx (e^{t\tau K_y^{(1)}} e^{t\tau K_y^{(2)}}) \otimes (e^{t\tau K_x^{(1)}} e^{t\tau K_x^{(2)}}) \equiv \widehat{B} \end{aligned} \tag{2.3.10}$$

There are 16 nonzero elements in every row and column of the matrix $\widehat{B}$. Therefore, if $\cosh\alpha$ and $\sinh\alpha$ are computed in advance, the cost to construct the the matrix $\widehat{B}$ is $16N$.

Note the the approximation (2.3.10) of B is not symmetric. A symmetric approximation of B is given by

$$\widehat{B} = (e^{\frac{t\tau}{2} K_y^{(2)}} e^{t\tau K_y^{(1)}} e^{\frac{t\tau}{2} K_y^{(2)}}) \otimes (e^{\frac{t\tau}{2} K_x^{(2)}} e^{t\tau K_x^{(1)}} e^{\frac{t\tau}{2} K_x^{(2)}}).$$

In this case, there are 36 nonzero elements in every row and column.

Matrix-vector multiplication. Let us consider the computation of the matrix-vector multiplication $\widehat{B}x$. Let x be a vector of the dimension $N = N_x \times N_y$ and X be an $N_x \times N_y$ matrix, such that

$$x = \mathrm{vec}(X).$$

Then we have

$$\widehat{B}x = \mathrm{vec}(e^{t\tau K_x^{(2)}} e^{t\tau K_x^{(1)}} X e^{t\tau K_y^{(1)}} e^{t\tau K_y^{(2)}}). \tag{2.3.11}$$

It can be verify that the cost of the matrix-vector multiplication $\widehat{B}x$ is $12N$. It can be further reduced by rewriting the block $e^{\alpha D}$ as

$$e^{\alpha D} = \cosh\alpha \begin{bmatrix} 1 & \tanh\alpha \\ \tanh\alpha & 1 \end{bmatrix}.$$

Using this trick, the cost of the matrix-vector multiplication $\widehat{B}x$ is $9N$.

2.4 Eigenvalue distribution of M

The study of eigenvalues of a cyclic matrix can be traced back to the work of Frobenius (1912), Romanovsky (1936) and Varga (1962). The following theorem characterizes the eigenvalue distribution of the Hubbard matrix M.

Theorem 2.4.1 *For each eigenpair (μ, w) of the matrix $B_L \cdots B_2 B_1$, there are L corresponding eigenpairs $(\lambda_\ell^M, v_\ell^M)$ of the matrix M given by*

$$\lambda_\ell^M = 1 - \lambda_\ell \quad \textit{and} \quad v_\ell^M = \begin{bmatrix} (B_L \cdots B_3 B_2)^{-1} \lambda_\ell^{L-1} w \\ (B_L \cdots B_3)^{-1} \lambda_\ell^{L-2} w \\ \vdots \\ B_L^{-1} \lambda_\ell w \\ w \end{bmatrix}$$

where

$$\lambda_\ell = \mu^{\frac{1}{L}} e^{\mathbf{i} \frac{(2\ell+1)\pi}{L}},$$

for $\ell = 0, 1, \ldots, L-1$.

The theorem can be verified by checking $(I - M) v_\ell^M = \lambda_\ell v_\ell^M$.

2.4.1 The case $U = 0$

When the Hubbard system without Coulomb interaction, $U = 0$, we have

$$B_1 = B_2 = \cdots = B_L = B = e^{t\tau K}.$$

In this case, the eigenvalues of the matrix M are known explicitly.

Theorem 2.4.2 *When $U = 0$, the eigenvalues of the matrix M are*

$$\lambda(M) = 1 - e^{t\tau \kappa_{ij}} e^{\mathbf{i} \frac{(2\ell+1)\pi}{L}}, \tag{2.4.12}$$

for $0 \le \ell \le L-1$, where κ_{ij} is defined in (2.3.8). Furthermore,

$$\max |1 - \lambda(M)| = e^{4t\tau} \quad \textit{and} \quad \min |1 - \lambda(M)| = e^{-4t\tau}.$$

The following plot shows the eigenvalue distributions of the matrix M with the parameters

$$N = 4 \times 4, L = 8, U = 0, \beta = 1, t = 1.$$

The dimension of the matrix M is $NL = 4 \times 4 \times 8 = 128$. Theorem 2.4.2 can be used to interpret the distribution. It has a ring structure, centered at $(1, 0)$. On every ring there are $L = 8$ circles. We can also view the eigenvalues distribute on $L = 8$ rays, centered at $(1, 0)$. The eigenvalues κ_{ij} of the matrix K only have 5 different values. There are total 40 circles, with some multiple eigenvalues.

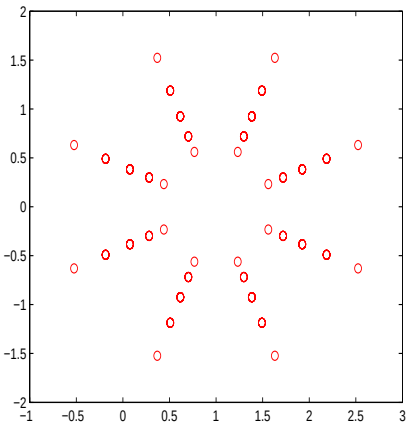

Let us examine the eigenvalue distributions of M under the variation of the parameters N, L, U and t.

1. Lattice size N: the following plot shows the eigenvalue distributions when $N = 4 \times 4$ and $N = 16 \times 16$. Other parameters are set as $U = 0$, $L = 8$ and $t = 1$. Note that there are more points on each ray, due to the fact that there are different values of κ_{ij} when $N = 16 \times 16$ than $N = 4 \times 4$.

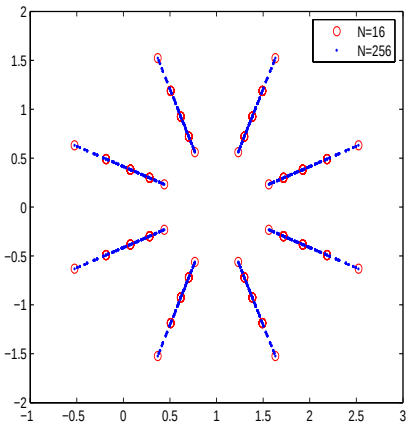

2. Block number L: the following plot shows the eigenvalue distribution for block numbers $L = 8$ and $L = 64$. Other parameters are set as $N = 4 \times 4$, $U = 0$ and $t = 1$. As we observe that as L increases, the number of rays increases, and the range of the eigenvalue distribution on each ray shrinks and becomes more clustered.

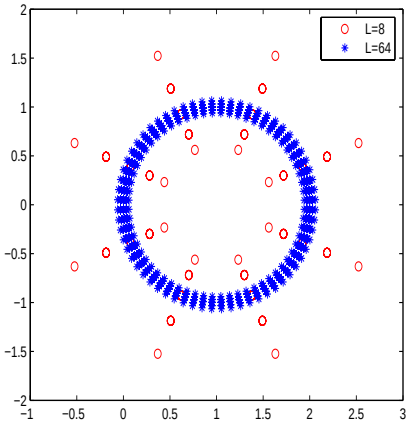

3. Block number L and t: the following plot shows the eigenvalue distributions for different pari $(L,t) = (8,1)$ and $(64,8)$. Other parameters are set as $N = 4 \times 4$ and $U = 0$. By Theorem 2.4.2, we know that the points on the one ring are equal to L. When L increases, the points on each ring increase. At the same time, since $\tau = \frac{1}{L}$, the range of $|1 - \lambda(M)|$ is $[e^{-\frac{4t}{L}}\ e^{\frac{4t}{L}}]$, the range will shrink when L increases. If we fix $\frac{t}{L}$, the range will still keep same. This is shown in the plot.

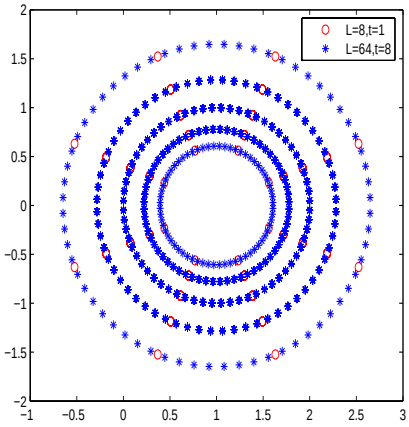

2.4.2 The case $U \neq 0$

Unfortunately, there is no explicit expression for the eigenvalues of the matrix M when $U \neq 0$. The following plot shows that as U increases, the range of eigenvalues on each ray is widen. Other parameters are set as $N = 4 \times 4, L = 8, t = 1$.

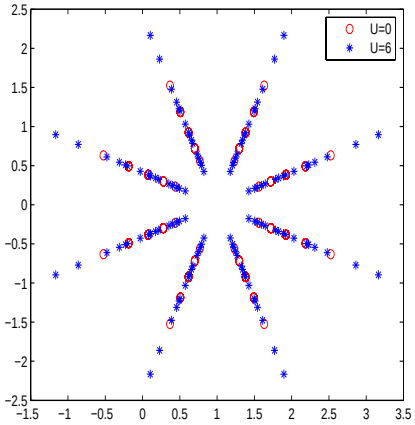

2.5 Condition number of M

In this section, we study the condition number of the Hubbard matrix M defined in (2.1.1).

2.5.1 The case $U = 0$

When $U = 0$, M is a deterministic matrix and furthermore, $B_1 = B_2 = \cdots = B_L = e^{t\tau K} \equiv B$. First, we have the following lemma about the the eigenvalues of the matrix $M^T M$.

Lemma 2.5.1 *When $U = 0$, the eigenvalues of $M^T M$ are*

$$\lambda_\ell(M^T M) = 1 + 2\lambda(B)\cos\theta_\ell + (\lambda(B))^2, \tag{2.5.13}$$

where

$$\theta_\ell = \frac{(2\ell+1)\pi}{L}$$

for $\ell = 0, 1, \cdots, L-1$.

The result is based on the following fact. For any real number a, the eigenvalues of the matrix

$$A(a) = \begin{bmatrix} 1+a^2 & -a & & a \\ -a & 1+a^2 & -a & \\ & \ddots & \ddots & \ddots \\ a & & -a & 1+a^2 \end{bmatrix}.$$

are

$$\lambda(A(a)) = 1 - 2a\cos\theta_\ell + a^2.$$

Note that for any real number a,

$$\sin^2\theta \le 1 - 2a\cos\theta + a^2 \le (1+|a|)^2,$$

Therefore, we have the following inequalities

$$\max\lambda_\ell(M^T M) \le (1 + \max|\lambda(B)|)^2 \quad \text{and} \quad \min\lambda_\ell(M^T M) \ge \sin^2\frac{\pi}{L}.$$

By these inequalities, the norms of M and M^{-1} are bounded by

$$\|M\| = \max \lambda_\ell (M^T M)^{\frac{1}{2}} \leq 1 + \max |\lambda(B)|,$$

and

$$\|M^{-1}\| = \frac{1}{\min \lambda_\ell (M^T M)^{\frac{1}{2}}} \leq \frac{1}{\sin \frac{\pi}{L}}. \tag{2.5.14}$$

Note that $B = e^{t\tau K}$ and $\lambda_{\max}(K) = 4$, we have the following upper bound of the condition number $\kappa(M)$ of M.

Theorem 2.5.1 *When $U = 0$,*

$$\kappa(M) = \|M\| \, \|M^{-1}\| \leq \frac{1 + e^{4t\tau}}{\sin \frac{\pi}{L}} = \mathcal{O}(L). \tag{2.5.15}$$

Therefore, when $U = 0$, the matrix M is well-conditioned.

2.5.2 The case U is sufficient small

We now consider the situation when $U \neq 0$. By the representation of M in (2.1.3), we have

$$\|M\| \leq 1 + \max_\ell \|B_\ell\| \, \|P\| = 1 + \max_\ell \|B_\ell\| \leq 1 + e^{4t\tau + \nu}. \tag{2.5.16}$$

where $\cosh \nu = e^{\frac{U\tau}{2}}$, or approximately, $\nu \approx (\tau U)^{1/2}$.

To bound $\|M^{-1}\|$, we first consider when U is small. In this situation, we can treat the matrix M as a small perturbation of the matrix M at $U = 0$. We have the following result.

Theorem 2.5.2 *If U is sufficient small such that*

$$e^\nu < 1 + \sin \frac{\pi}{L}, \tag{2.5.17}$$

then

$$\kappa(M) = \|M\| \, \|M^{-1}\| \leq \frac{1 + e^{4t\tau + \nu}}{\sin \frac{\pi}{L} + 1 - e^\nu}.$$

PROOF: M can be expanded at $U = 0$, denoted by M_0:

$$M = M_0 + \mathrm{diag}(B - B_\ell)\Pi,$$

where $B = e^{t\tau K}$. Note that $\|\Pi\| = 1$, then if $\|M_0^{-1}\mathrm{diag}(B - B_\ell)\| < 1$, then we have

$$\|M^{-1}\| \leq \frac{\|M_0^{-1}\|}{1 - \|M_0^{-1}\mathrm{diag}(B - B_\ell)\|}. \tag{2.5.18}$$

Since Why???

$$\|M_0^{-1}\mathrm{diag}(B)\| \leq \frac{1}{\sin \frac{\pi}{L}},$$

we have

$$\|M_0^{-1}\mathrm{diag}(B-B_\ell)\| \le \|M_0^{-1}\mathrm{diag}(B)\|\|\mathrm{diag}(I-e^{V_\ell})\| \le \frac{e^\nu-1}{\sin\frac{\pi}{L}}.$$

Now, if

$$\frac{e^\nu-1}{\sin\frac{\pi}{L}} < 1$$

i.e,

$$e^\nu < 1+\sin\frac{\pi}{L},$$

by (2.5.18) and (2.5.14), we have

$$\|M^{-1}\| \le \frac{\frac{1}{\sin\frac{\pi}{L}}}{1-\frac{e^\nu-1}{\sin\frac{\pi}{L}}} = \frac{1}{\sin\frac{\pi}{L}+1-e^\nu}.$$

This completes the proof. ∎

Note that the Taylor expansion of ν gives the expression

$$\nu = \sqrt{U\tau} + \frac{(U\tau)^{\frac{3}{2}}}{12} + O(U^2\tau^2). \tag{2.5.19}$$

Then to the first-order approximation, the conditon (2.5.17) is

$$\sqrt{U} \le \frac{\pi}{\beta}\sqrt{\tau} + O(\tau), \quad \text{or} \quad U \le \frac{\pi^2}{\beta^2}\tau + O(\tau^{\frac{3}{2}}). \tag{2.5.20}$$

Therefore, to the first order approximation, we have

$$\kappa(M) \le \frac{L(1+e^{4t\tau+\nu})}{\pi-\beta\sqrt{U\tau}-U\beta/2} + O(U^{\frac{3}{2}}\beta\tau^{\frac{1}{2}}).$$

By the inequality, we conclude that when U is sufficient small enough, M is well-conditioned and $\kappa(M) = \mathcal{O}(L)$.

2.5.3 The case $U =\neq 0$

In general, it is still an open problem for a rigorous sharp upper bound $\kappa(M)$ for general $U \neq 0$. The following plot shows the averages of the condition numbers of M for 100 H-S field configurations $h_{\ell,i} = \pm 1$, uniform two-point distribution, where $N = 16$, $L = 8\beta$ with $\beta = [1:10]$, and $t = 1$.

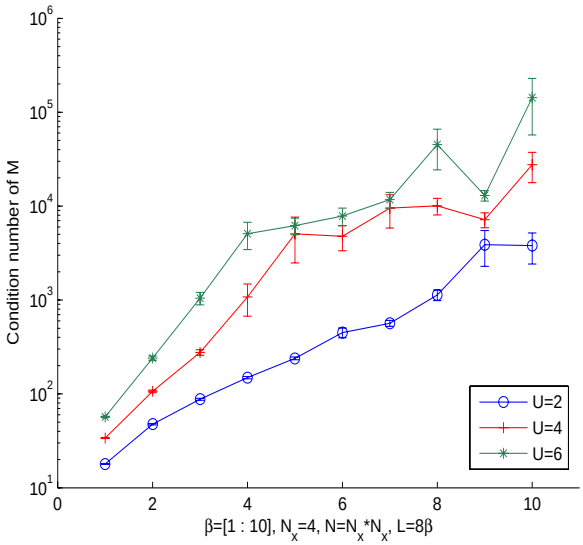

The above plot reveals two key issues concerning the transition from well-conditioned to ill-conditioned behaviors:

1. When $U \neq 0$, the condition number increases much more rapidly than the linear rise which we know analytically at $U = 0$.

2. Not only does the condition number increase with U, but also so do its fluctuations over the 100 chosen field configurations.

The first observation tells us the parameter L is critical to the difficult of our numerical linear algebra solvers. The second suggests that widely varying condition number might be encountered in the course of a simulation, and therefore that a solver might need to have the ability to adopt different solution strategies on the fly.

2.6 Condition number of $M^{(k)}$

For an integer $k \leq L$, a structure-preserving factor-of-k reduction of the matrix M leads a matrix $M^{(k)}$ of the form

$$M^{(k)} = \begin{bmatrix} I & & & & B_1^{(k)} \\ -B_2^{(k)} & I & & & \\ & -B_3^{(k)} & I & & \\ & & \ddots & \ddots & \\ & & & -B_{L_k}^{(k)} & I \end{bmatrix}.$$

where $L_k = \lceil \frac{L}{k} \rceil$ is the number of blocks and

$$\begin{aligned} B_1^{(k)} &= B_k B_{k-1} \cdots B_2 B_1 \\ B_2^{(k)} &= B_{2k} B_{2k-1} \cdots B_{k+2} B_{k+1} \\ &\vdots \\ B_{L_k}^{(k)} &= B_L B_{L-1} \cdots B_{(L_k-1)k+1}. \end{aligned}$$

First we have the following observation: the inverse of $M^{(k)}$ is a "submatrix" of the inverse of M. Specifically, since M and $M^{(k)}$ have the same block cyclic structure, by the expression (2.2.6), we immediately have the following expression for the (i,j) block of $\{M^{(k)}\}_{i,j}^{-1}$:

$$\{M^{(k)}\}_{i,j}^{-1} = (I + B_i^{(k)} \cdots B_1^{(k)} B_L^{(k)} \cdots B_{i+1}^{(k)})^{-1} Z_{i,j}^{(k)}$$

where

$$Z_{i,j}^{(k)} = \begin{cases} B_i^{(k)} B_{i-1}^{(k)} \cdots B_{j+1}^{(k)}, & i > j \\ I, & i = j \\ -B_i^{(k)} \cdots B_1^{(k)} B_L^{(k)} \cdots B_{j+1}^{(k)}, & i < j \end{cases},$$

By the definition of $B_i^{(k)}$, and if $i \neq L^{(k)}$

$$\{M^{(k)}\}_{i,j}^{-1} = (I + B_{ik} \cdots B_1 B_L \cdots B_{i*k+1})^{-1} \begin{cases} B_{i*k} \cdots B_{j*k+1}, & i > j \\ I, & i = j \\ -B_{i*k} \cdots B_1 B_L \cdots B_{j*k+1}, & i < j \end{cases}.$$

Hence if $i \neq L^{(k)}$,

$$\{M^{(k)}\}_{i,j}^{-1} = \{M^{-1}\}_{i*k,j*k}.$$

If $i = L^{(k)}$, we have

$$\{M^{(k)}\}_{i,j}^{-1} = (I + B_L \cdots B_1)^{-1} \begin{cases} B_L \cdots B_{j*k+1}, & j < L \\ I, & j = L \end{cases}.$$

Hence if $i = L^{(k)}$,

$$\{M^{(k)}\}_{L^{(k)},j}^{-1} = \{M^{-1}\}_{L,j*k}.$$

We now turn to the discussion of the condition number of the matrix $M^{(k)}$. We have the following two immediate results:

1. Since an upper bound of the norm of the matrix $B_\ell^{(k)}$ is given by

   $$\|B_\ell^{(k)}\| \leq e^{(4t\tau+\nu)k}.$$

   we have

   $$\|M^{(k)}\| \leq 1 + e^{(4t\tau+\nu)k}. \tag{2.6.21}$$

2. Since $(M^{(k)})^{-1}$ is a "submatrix" of M^{-1}, we have

   $$\|(M^{(k)})^{-1}\| \leq \|M^{-1}\|. \tag{2.6.22}$$

By combining (2.6.21) and (2.6.22), we have

$$\begin{aligned}\kappa(M^{(k)}) &= \|M^{(k)}\|\,\|(M^{(k)})^{-1}\| \\ &\leq \frac{\|M^{(k)}\|}{\|M\|}\|M\|\|M^{-1}\| = \frac{\|M^{(k)}\|}{\|M\|}\kappa(M) \\ &\leq \frac{1+e^{(4t\tau+\nu)k}}{\|M\|}\kappa(M).\end{aligned}$$

In summary, we have

$$\kappa(M^{(k)}) \leq ce^{(4t\tau+\nu)k}\kappa(M), \tag{2.6.23}$$

where c is some constant. It shows that the condition number of $M^{(k)}$ is bounded by the product of the condition number of M and a quantity involving reduction factor k.

For further details, let us first examine the case where $U = 0$ and the reduction factor $k = L$. In this case, the matrix M is reduced to a single block

$$M^{(L)} = I + B_L \cdots B_2 B_1 = I + B \cdots BB = I + B^L = I + (e^{t\tau K})^L = I + e^{t\beta K}.$$

Then the condition number of $M^{(L)}$ is given by the eigendecomposition of the matrix K:

$$\kappa(M^{(L)}) = \frac{1+e^{4t\beta}}{1+e^{-4t\beta}}.$$

Note that $M^{(L)}$ is extremely ill-conditioned when β is large.

When $U = 0$ and the reduction factor $k < L$, and $L_k = \frac{L}{k}$ is an integer, then we have the following result

$$\kappa(M^{(k)}) \leq \frac{1+e^{4t\tau k}}{\sin\frac{\pi}{L_k}}.$$

The inequality can be proved in a similar way as the proof of Lemma 2.5.1. We believe the bound is still true even when L/k is not an integer. The following figure shows condition numbers of $M^{(k)}$ with respect to the reduction factor k when $U = 0$. The computational and estimated results fit well.

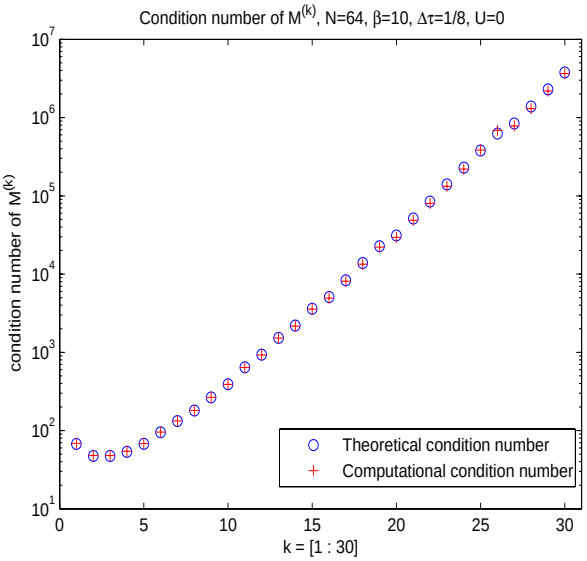

In general, when $U \neq 0$, we have the bound (2.6.23). The following figure shows the condition numbers of a few sample matrices $M^{(k)}$ (solid lines), and the upper bound (2.6.23) (circle dashed line). for $U = 4$ and $U = 6$. The condition number $\kappa(M)$ of M uses the mean of the condition numbers of the sample matrices M.

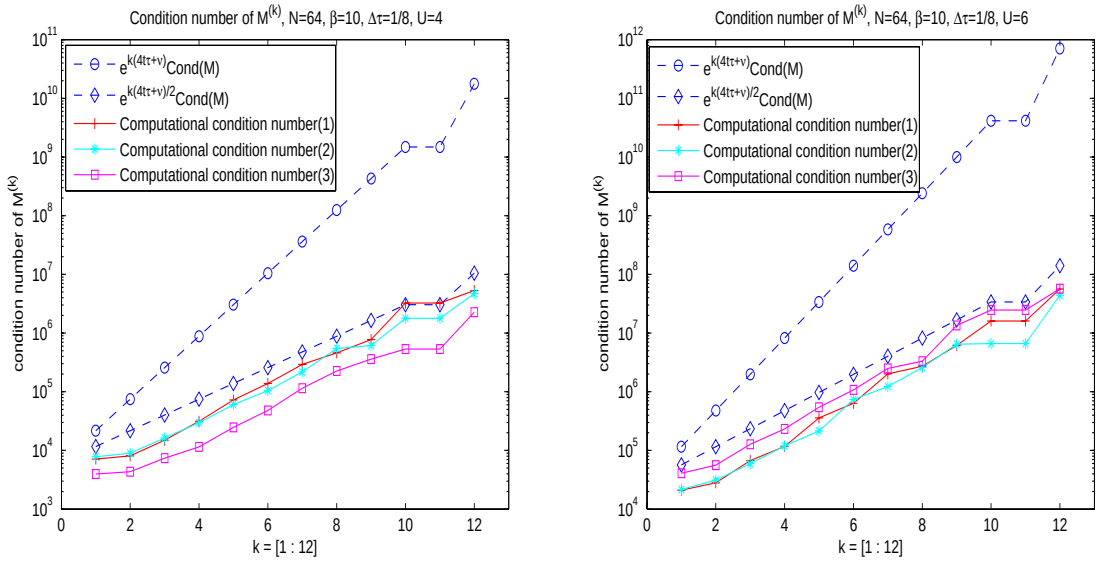

It is clear that the upper bound $e^{k(4t\tau+\nu)}\kappa(M)$ is overestimated, partially due to the overestimation of the norm of $M^{(k)}$. We observe that the condition number of $M^{(k)}$ is closer to the quantity $\sqrt{e^{k(4t\tau+\nu)}}\kappa(M)$, shown as the diamond dashed line of the plots. This is a subject of further study.